Technische Universität München
TUM School of Medicine and Health

18F-rhPSMA7 for biochemical recurrence in prostate cancer

Lena Charlotte Ulbrich

Vollständiger Abdruck der von der TUM School of Medicine and Health der Technischen Universität München zur Erlangung einer

Doktorin der Medizin (Dr.med.)

genehmigten Dissertation.

Vorsitz: apl. Prof. Dr. Bernhard Haslinger

Prüfende der Dissertation:

1. *Prof. Dr. Tobias Maurer*
2. *apl. Prof. Dr. Matthias Eiber*

Die Dissertation wurde am 05.10.2023 bei der Technischen Universität München eingereicht und durch die TUM School of Medicine and Health am 06.02.2024 angenommen.

18F-rhPSMA7 for biochemical recurrence in prostate cancer

Detection of biochemical recurrence of prostate cancer following radical prostatectomy through 18F-rhPSMA-7 positron emission tomography

Lena Ulbrich

Abreviations alphabetical

225Ac:	225-Actinium
ADC:	Apparent Diffusion Coefficient
ADT:	Androgen Deprivation Therapy
AS:	Active Surveillance
BCR:	Biochemical Recurrance
CAB:	Complete Androgen Blockage
CT:	Computer Tomography
DCE:	Dynamic Contrast Enhanced
DRE:	digital rectal examination
DWI:	Diffusion Weighted Imaging
EBRT:	External Beam Radiation Therapy
ePLND:	external Pelvic Lymph Node Dissection
68Ga:	68-Gallium
GS:	Gleason Score
HIFU:	High Intensity Focused Ultrasound
HTX:	Hormonal Therapy
IARC:	International Agency for research on Cancer
ISUP:	International Society of Urologic Pathology
18FDG:	18-Flourdesoxyglucose
19F:	19-Flourine
177LU:	177-Lutetium
Mab:	Monoklonal Antibody
MP-MRI:	Multiparametric-MRI
MRI:	Magnet Resonant Imaging
NPV:	Negative Predictive Value
PC:	prostate cancer
PET:	Positron Emission Tomography
PPV:	Positive Predictive Value
PSA:	Prostate Specific Antigen
PSAdt:	Prostate Specific Antigen doubling time
PSAvel:	Prostate Specific Antigen velocity
PSM:	Positive Surgical Margins
PSMA:	Prostate Specific Membrane Antigen

RP:	Radical Prostatectomy
RTx:	Radiotherapy
rh:	Radiohybrid
SIFA:	Silicon Flouride Acceptor
SPECT:	Single Photon Emission Computet Romgraphy
SRT:	Salvage Radiotherapy
TRUS:	transrectal ultrasound
WW:	Watchful waiting

List of figues

List of tables

1. Introduction

1.1 Epidemiology

With 1.4 million diagnoses worldwide in 2020 according to the International Agency for research on Cancer (IARC) prostate cancer (PC) is the second most frequently diagnostized cancer and the fifth most frequent cause of cancer deaths among men (Bray et al., 2018). With 20%, PC has the highest 5-year prevalence rate among all cancers. Genetic predisposition such as race and familial accumulation, molecular changes, chronic inflammation, testosterone and environmental factors play a role in the epidemiology of PC.

There is variation of incidences due to underdiagnosis in developing countries and overdiagnosis, especially in the USA and Europe, differences in the screening methods and disparities in healthcare access. Mortality, however, is less affected by those differences. Most of all, age rises the incidence and mortality rate of PC, therefore 55% af all deaths occure at the age above 65 years. The IARC states that in 2020 rates are generally high in population of Europe, followed by Asia and Northern America. (Bray et al., 2018)

1.2 Primary Detection

Since PC does not cause any symptoms in the early stages it is difficult to detect the disease early and treat it successfully. Despite the constant improvement of the understanding of PC and the earlier detection of the disease through new diagnostic methods, it remains the second most cause of cancer deaths among men in the USA (Baade et al., 2009).

In industrialized countries, PC nowadays is often diagnosed by an elevated PSA (Prostate specific antigen) level in the blood, which is organ but not cancer

specific. However, it is still more accurate than digital rectal examination (DRE) or transrectal ultrasound (TRUS) of the prostate (Catalona et al., 1994). Nevertheless, even in healthy men there are elevated PSA levels, so that DRE, tissue biopsy and histological confirmation remain the standard of diagnosis (Rawla, 2019).

Gleason score (GS) is the most commonly used grading for PC. It is based on the assessment of gland morphology at relatively low magnification. The cytological properties of the cells are not evaluated. A Gleason pattern with values between 1-5 is assigned to the different existing gland architectures. The predominant and the worst differentiated Gleason grade are combined to a GS. This score can be 2 (1+1) to 10 (5+5). The GS correlates with the prognosis of the tumor. Poor prognostic signs in the punch biopsy can usually also be verified in the surgical preparation. More problematic is the underestimation of the tumor disease. 40% of patients with Gleason Score 5 or 6 in the punch biopsy have a higher GS in the surgical preparation. 40% of patients with only one affected prostate punch have extraprostatic tumor growth (T3) (Epstein et al., 2005).

PC most commonly spreads into lymph nodes and bones. Over the last two decades imaging methods like MRI (magnetic resonance imaging) and CT (computer tomography) have been used to improve tumor localisation and staging in primary and recurrent disease (Eiber et al., 2017). However, those imaging strategies depend on non-specific size criteria to define possible malignant lymph nodes despite 80% of lymph node metastases not meeting the standard of 8 mm threshold. Extended pelvic lymph node dissection (ePLND) therefore remains the gold standard for lymph node staging in PC. However, operative management is not an option for all patients. Furthermore, ePLND

can be associated with an overall complication rate of up to 20% (Rahman et al., 2019).

1.3 Primary therapy

The primary therapy can consist of one or a combination of five therapy pillars:

- Deferred treatment like active surveillance (AS) for low risk patients and a life expectancy above 10 years or watchful waiting (WW), with a palliative intent for patients of all cancer stages but a life expectancy below 10 years due to their comorbidities. These two conservative managements of the disease aim to reduce overtreatment.
- Radical prostatectomy (RP), the complete removal of the prostate, including capsule and seminal vesicles and depending on the cancer stage also of the regional lymph nodes, with the goal of eradicating the cancer as well as to preserve potency and continence. A therapy which is widly used but comes with possibly severe side effects like incontinence or erectile dysfunction.
- Radiotherapy (RTX), like external beam radiation therapy (EBRT) and brachytherapy, which both show no difference to RP regarding oncological outcomes.
- Hormonal therapy (HTX) including the supression of androgen synthesis or inhibiting their action by blocking the androgen receptors. In combination known as a complete androgen blockage (CAB).

In addition there are investigational therapies, i.e. focal therapy including cryotherapy or high intensity focused ultrasound.

The choice of treatment depends on the wishes of the patient, the state of the disease, based on PSA-value and kinetics, the GS and the objectives, regarding life expectancy and comorbidities (Cornford et al., 2017).

1.4 Biochemical recurrence of prostate cancer

After RP, 27% to 53% of patients are faced with the biochemical recurrence of the PC, diagnosed through a rising serum-PSA (Van den Broeck et al., 2019). According to the German S3-guidelines the definition of BCR is a PSA above 0.2 ng/ml, confirmed in at least two measurements of two weeks apart after RP (Stephenson et al., 2006).

Short latency of the PSA-relapse, increased PSA-kinetics like a short PSA-doubling time (PSAdt) <3 month, high PSA-velocity (PSAvel) and GS >7, positive surgical margins or high RP specimen pathological ISUP (International Society of Urologic Pathology) grade and high pT category correlate with an increased risk of a systemic recurrence and therefore an unfavorable prognosis. Local recurrence seems to be characterized by later BCR, a longer PSAdt and lower GS (Cornford et al., 2017).

Figure 1: ISUP risk group stratification

Risk group of BCR	
Low-risk BCR	PSAdt >1year and pGS <8 (ISUP grade <4)
High-risk BCR	PSAdt <1year or pGS 8–10 (ISUP grade 4–5)

pGS = pathological Gleasonscore; ISUP=International Society of Urological Pathology;

IBF=interval from primary therapy to biochemical failure; bGS = biopsy Gleasonscore (Van den Broeck et al., 2019).

All these variables are not fully reliable, especially at low PSA levels and not every man with BCR will develop progressive disease, including symptoms or evidence of such (Van den Broeck et al., 2019).

Nonetheless, BCR is associated with oncological endpoints like clinical failure, PC-specific mortality, and overall mortality, with range of effect varying across studies. Adequate life expectancy is crucial for treatment decision as the median actuarial time to development of metastasis is 8 years and the median time from metastasis to death is a further 5 years (Van den Broeck et al., 2019).

1.4.1 Treatment of BCR

There are different approaches for the treatment of BCR after RP depending on the dimension of the progress of the disease.

For asymptomatic patients 'watchful waiting' might be suitable. A palliative systematic therapy is usually indicated when the PC has symptomatically metastasized and serves as basis to slow down disease progression and to maximize quality of life. Androgen deprivation therapy (ADT) or chemotherapy to alleviate symptoms as well as adequate pain relieve are also indicated.

In case of local recurrence, salvage RTX of the prostate fossa with curative intent is recommended by the European and German guidelines as early as possible (PSA < 1ng/mL). Since sensitivity for anastomotic biopsies is low especially at low PSA- levels histological confirmation is not recommended (Cornford et al., 2021). The combination of ADT and salvage radiotherapy (SRT) showed a reduction in distant metastasis only in patients with aggressive disease characteristics (pT3b/4 and ISUP grade > 4 or pT3b/4 and PSA at early SRT > 0.4 ng/mL) (Cornford et al., 2021).

1.4.2 Imaging of BCR after RP

The evaluation of men with asymptomatic BCR after RP benefits from the development of new clinical tools that provide better risk stratification to assess the risk of metastasis. Risk calculators and nomograms help urologists and patients estimate the likelihood of developing metastatic disease and experiencing cancer-specific mortality in the future. This can lead to earlier intervention in the adjuvant or salvage setting. Above all, it can help to avoid overtreatment of men at low risk of progressive disease. Still, the more difficult task is to locate the specific sites of disease recurrence.

Compared to other imaging modalities, multiparametric MRI (MP-MRI) provides the best anatomical visualization of the prostate due to its superior spatial and contrast resolution. High field strength magnets and special coil designs result in a higher signal-to-noise ratio, and thus increase resolution, contrast, and/or speed, and outperform other techniques in delineating intraprostatic tumor sites. The most optimal technique involves a multiparametric approach that includes anatomical and functional sequences. The method can be performed with 1.5 T and 3.0 T MR tomographs and adds up to 3 different MR sequences and thus examination parts.

T2-weighted MR sequences (T2w) to assess morphology: this sequence is used to detect structural features of the prostate, seminal vesicles and surrounding organs/tissues and also to perform local staging.

Diffusion-weighted MR sequences (DWI) visualize areas of increased cell density, typical of a PC. Compared to normal glandular tissue, it contrasts signal-rich on the high diffusion weighting images and signal-poor on the

corresponding apparent diffusion coefficient (ADC) parameter maps. This MR sequence is critical for the detection and characterization of prostate cancer.
Dynamic contrast enhanced (DCE) MR sequences depict increased tissue perfusion/tumor neovascularization: After intravenous administration of a gadolinium-containing contrast agent, the PC contrasts with an early arterial and strong signal intensity increase.
The diagnosis of prostate cancer is still a histopathological one and is based on information such as age, PSA parameters, prostate size and presence of benign prostate disease, concomitant diseases, etc.

To provide a target orientated treatment in case of BCR, imaging seems to be imperative and should open the way to focal salvage treatments in the near future. As mentioned above, early detection and accurate localization of any local recurrence or residuals of malignant tissue as well as metastases would be crucial for better outcome, cancer related and overall mortality.
Nevertheless, imaging such as bone scintigraphy, computer tomography (CT), MRI, X-ray is not part of the EAU- or German S3-guidelines recommendations as patients should be spared unnecessary examinations based on lack of sensitivity at low PSA levels (Kane et al., 2003). Therapeutic consequences are the only indication for use of imaging in case of BCR. Imaging for a pure follow-up would not be justifiable at this stage of the disease. According to the guidelines indications for imaging are increasing symptoms, change in the general condition and/or newly occurring symptoms that may require further treatment (Cornford et al., 2021).

1.4.2.1 Positron emission tomography

Positron emission tomography (PET) is an imaging technique used in nuclear medicine. PET produces sectional images of living organisms by making the distribution of a weakly radioactively labelled substance (radiopharmaceutical) in the organism visible, thus producing functional imaging. PET can answer questions regarding metabolic processes like glucose metabolism, receptor status or surface antigen properties like PSMA status (Glatting et al., 2017).

It is based on the simultaneous detection of two gamma radiation photons which are produced after the decay of a positron emitting radionuclide (Glatting et al., 2017).

The positrons emitted in the body have a short lifetime of nanoseconds and interact with an electron almost instantaneously. This produces secondary annihilation radiation, in which two high-energy photons of 511 keV are emitted in at an angle of 180 degrees to each other. The PET detectors are arranged in a ring around the patient. Only those decay events are counted that are based on exact coincidences between each two opposite detectors. From the temporal and spatial distribution of these decay events, the spatial distribution of the radiopharmaceutical location is deduced, and a series of sectional images is calculated. This results in a primarily functional CT-image.

Figure 2: PET-CT principle(metaversexsyasian.blogspot.com)

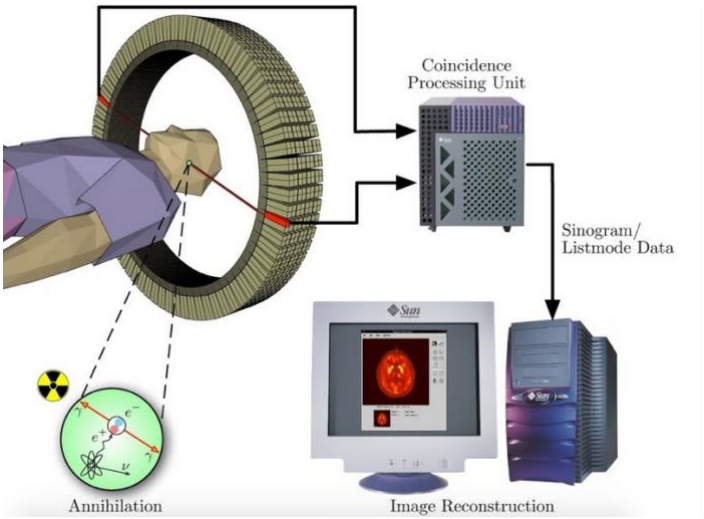

1.4.2.2 PET/CT imaging

The CT scan is usually performed first and followed by the PET scan and then connected to it. The image reconstruction starts as soon as the image of the first bed position is complete. In some systems, the gantries are located in the same housing. The calculated images are automatically fused in the computer (Glatting et al., 2017).

Even though PET is highly sensitive depending on the question, anatomically correct localization of activity accumulations can be difficult since PET images primarily show metabolic processes; in addition, there is the limited spatial resolution of about 4-6 mm. The high spatial resolution of up to 0.35 mm and detailed anatomical representation of the CT with the highly sensitive functional information from the PET is combined in a PET/CT since 2001 (Hentschel et al., 2007). In PET/CT, the patient is moved through both detector rings of CT and PET right after each other. The CT data is required to reconstruct the PET data.

1.4.2.3 Prostate Specific Membrane Antigen-based imaging

Prostate specific membrane antigen (PSMA), Glutamate carboxypeptidase II, also known as N-acetyl-L-aspartyl-L-glutamate peptidase I, is a 750-amino acid, 100kDA class II membrane glycoprotein which catalyzes the hydrolysis of N-acetylaspartylglutamate to glutamate and N-acetylaspartate. It is expressed in different tissues like the prostate, kidneys, small intestine, central and peripheral nervous system and tumor-associated neovasculature. (Barinka et al., 2004). The PSMA-gene is located on the short arm of chromosome 11. Even though PSMA is also found in other cancerous cells like named above, in differentiated and metastatic prostate cells it is upregulated the most with up to 100-1000 times higher than usual and correlates well with serum PSA concentration (Afshar-Oromieh et al., 2017; Lin et al., 2020; Troyer et al., 1995, 1997).

Despite the fact, that no natural ligand for PSMA as well as the reasons for its upregulation in PC is known, the ligand undergoes cell internalization by PSMA, from the apical side to the basolateral membrane of the prostatic duct cells. Therefore, it seems to be an appealing target for imaging in metastatic PC regarding the high tumor to background ratio (Afshar-Oromieh et al., 2017; Haberkorn et al., 2016). Although 5–10% of PCs may not express PSMA, studies have demonstrated that 98% of lymph node metastases do (Rahman et al., 2019).

Figure 3 PSMA protein [22]

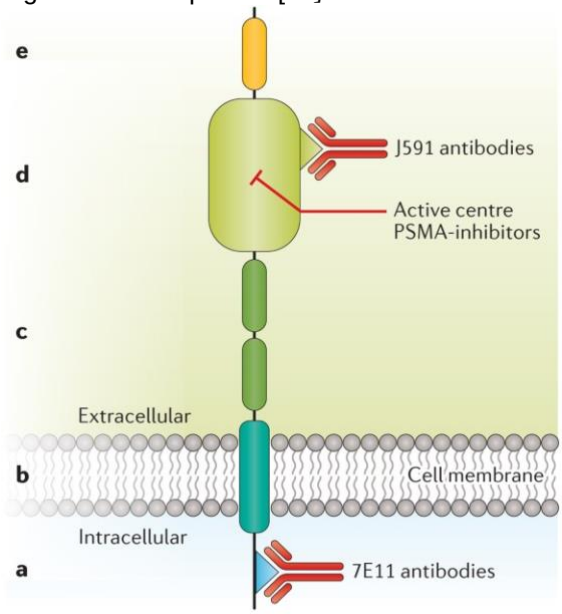

Domain with unknown function
Catalytic domain with junction for antibody and center for substrate recognition
Domains with unknown function
Hydrophobic transmembrane part
Short intracellular part with binding component for antibodies, 19 amino acids

The monoclonal antibody (MAb) 7E11 recognizes a PSMA epitope located on the cytoplasmic side of the differentiated prostate cell membrane and can bind to PSMA after the cell's apoptosis or necrosis (Horoszewicz et al., 1987; Troyer et al., 1995, 1997). The external membrane PSMA epitope is expected to bind on active prostate cancer cells. Consequently, a humanized antibody huJ591 (J591) that targets to the extra-cellular domain of PSMA was developed for imaging and therapy of prostate cancer (Christiansen et al., 2005; Holland et al., 2010). Additionally, it seems, that the PSMA levels are independent to the metabolism and the proliferation rate of the malignant cells. This seems to be an advantage regarding the slow growing rate of PC as well as the ability to differentiate Malignant grows from inflammatory tissue. This is a great advantage to the common 18-flourdesoxyglucose (18FDG) and cholin-derivates (Duwel et al., 2016). The overexpression of PSMA seems to be correlated to the severity of the disease.

1.4.2.4. Family of PSMA-Tracers

After approval by the U.S. Food and Drug Admin-istration in 1996 111In-labeled 7E11, 111In-Capromabpendetide (ProstaScint) has been investigated clinically for imaging recurrent and metastatic PC as a single photon emission computed tomography (SPECT) radiopharmaceutical (Petronis et al., 1998; Sodee et al., 2000). As mentioned above, intracellular epitopes are only accessible for necrotic or apoptotic cells, therefore the use of ProstaScint is limited for clinical diagnosis (Smith-Jones et al., 2003).

The humanized antibody J591 showed excellent tumor binding specificity in prostate cancer xenograft after extensive preclinical model studies and is currently the only Mab used for direct tumor cell radiotherapy. However, monoclonal antibodies are large constructs. Smaller molecules offer better tumor permeability and the advantage of faster blood clearance. PSMA inhibitors are smaller molecular entities, thus the current research efforts of radiopharmaceutical companies are focused on the development of these (Fernández-García et al., 2015; Lin et al., 2020).

Phosphorus-based compounds were the first ligands with high affinity for PSMA. However, due to the high polarity and relatively poor pharmacokinetic profiles of these compounds, their clinical applications are limited. Due to their increased membrane permeability and oral bioavailability, variants of the thiol-, hydroxamate-, and sulfonamide-containing compounds have been evaluated as alternatives but are hindered by their relatively low PSMA selectivity and metabolic stability. Subsequently, extensive structural activity studies were conducted, resulting in several urea-based ligands. Some are highly specific for PSMA and have therefore been further used for diagnostic and therapeutic purposes (Chakravarty et al., 2018; Ding et al., 2007; Jackson et al., 1996).

1.4.2.4.1 68-Gallium

68Ga is a short-lived radionuclide with a half-life of 68 minutes and decays mainly by positron emission. It was commercially made available for the first time in Russia about 20 years ago and opened new possibilities of 68Ga in preclinical and clinical applications. It is able to form stable complexes with chelators such as diethylenetriaminepentaacetic acid,1,4,7,10-tetraazacyclododecan-1,4,7,10-tetraacetic acid [DOTA]. These are already widely used for MRI and SPECT, and thus, especially after the first successful clinical study of 68Ga-DOTATOC in 2001, research with 68Ga has increased significantly (Hofmann et al., 2001). Since 2011, 68Ga-PSMA-11 (also called HBED-CC, HBED, PSMA-HBED, or Prostamedix) is clinically established. Multiple studies have compared 68Ga-PSMA-11 with other PET-tracers for imaging patients with PC. It detects recurrent and metastatic disease by binding to the extracellular domain of PSMA and being internalized as described above. It provides higher detection rates in comparison to data from literature and 18F-choline based tracers. For PSA categories 0-0.19, 0.2-0.49, 0.5-0.99, 1-1.99, and ≥2ng/mL in BCR patients after RP, the percentages of positive scans were 33%, 45%, 59%, 75%, and 95%, respectively shown in a study from 2020 (Afshar-Oromieh et al., 2017; Perera et al., 2016; Perera et al., 2020). Among all PSMA inhibitor-based radiopharmaceuticals, 68Ga-PSMA-11 might be the best investigated agent for PET imaging of PC so far and is an established imaging technique (Afshar-Oromieh et al., 2017; Maurer, Eiber, et al., 2016; Perera et al., 2020).

1.4.2.4.2 18F-labelled agents

When it comes to restaging of BCR, 18F-labelled PSMA-PET tracers are increasingly used and preferred over 68Ga-labelled-PSMA-11. Compared to the first generation (such as 18F-DCFBC (N-[N-[(S)-1,3-dicarboxypropyl]carbamoyl]-4-F-fluorobenzyl-L-cysteine)), the second generation of 18F-PSMA-PET tracers (such as 18F-DCFPyl) has five times stronger binding affinities, lower radiation exposure and significantly lower blood pool activity (Lindenberg et al., 2016). However, neither 18F-DCFBC nor 18F-DCFPyL includes a chelator capable of binding therapeutic nuclides (Giesel et al., 2017).

A 2020 study showed a high detection rate in patients with PC after radical treatment and low PSA levels in 18F-PSMA-1007 PET/CT, that has recently been introduced clinically. Again, the detection rate correlates with the level of the PSA-value. An excellent sensitivity of 100%, specificity of 94% negative predictive value (NPV) of 100% and positive predictive value (PPV) of 66% was shown (Witkowska-Patena et al., 2020). The nonurinary excretion could be advantageous in cases of local recurrence and unclear lesions near the ureter or urinary bladder (Giesel et al., 2018; Rahbar, Weckesser, et al., 2018).

18F-PSMA-1007 can be produced in large quantities on site using a cyclotron, making it more cost effective. Its longer half-life allows it to be transported to nuclear medical centres without the need for a cyclotron, making it accessible for a wider range. The reduced urine excretion and a high tumor to background ratio leads to an increased sensitivity even for very small tumor lesions (Giesel et al., 2017).

1.4.2.5 Radiohybrid PSMA-ligands

Radiohybrid PSMA tracers are new theranostic targeting agents in PC. The radiohybrid concept became clinically valuable when it was combined with a Silicon-Flouride Acceptor (SiFA) based tracer which allows a simple, fast, reliable and transferable labeling method. A chelator which can either be cold (natGa or natLu) for imaging purposes or radiometal (68Ga, 177Lu, 225Ac) for therapeutic applications is attached. Metal chelats like 18F compensate for the high lipophilicity of the SiFA and therefore reduce the uptake of the tracer in organ tissue. They have shown to be equal or better than previously used 18F-PSMA tracers as they are associated with lower positron range, longer half-lives and larger scale production compared with their 68Ga-labelled counterparts (Wurzer et al., 2020).

As they are monozygotic chemical twins, they come with the possibility to produce identical 68Ga-labeled 19F-68Ga -rhPSMA tracers at sites that favour 68Ga labelling and the possibility to extend this concept to theranostic radiohybrid radiopharmaceuticals (Wurzer et al., 2020).

Figure 4: Radiohybrid concept, Wurzer.eEt.al

A

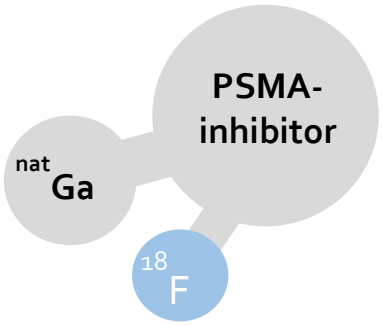

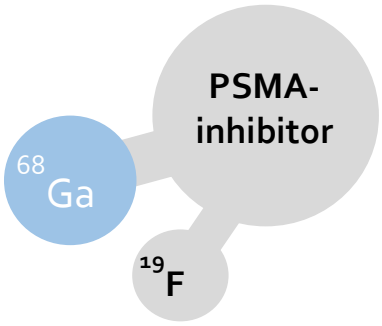

e.g. [^{18}**F**][^{nat}Ga]rhPSMA

[^{19}F]**[**^{68}**Ga]**rhPSMA

B

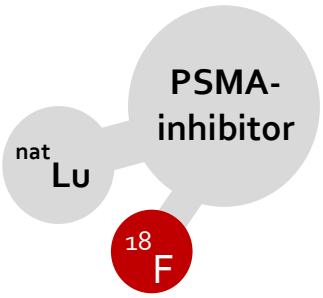

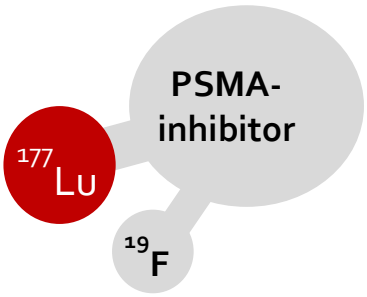

e.g. [^{18}**F**][^{nat}Lu]rhPSMA

[^{19}F]**[**^{177}**Lu]**rhPSMA

.

2. Questions and Aims

This retrospective analysis tries to elucitate the following questions:

- the use of 18F-PSMA7 in biochemical recurrant prostate cancer
- the corrolation between detection rate and PSA
- detection rate depending on prior EBRT, ADT within 6 months prior to imaging
- the localisation of recurrence in correlation with PSA level and the primary histological differentiation of the prostatectomy specimen

3. Material and Methods

3.1 Synthesis of 18F rhPSMA-7

Wurzer et. al. synthesised the rhPSMA ligands using a mixed solid phase/solution phase synthesis strategy, detailed in his paper 'Radiohybrid Ligands: A Novel Tracer Concept Exemplified by (18)F- or (68)Ga-Labeled rhPSMA Inhibitors'.

3.1.1 Following, the radiopharmaceutical detail of resynthesis for 18F-rhPSMA are described

Both Fmoc-(9-fluorenylmethoxycarbonyl-) and all other amino acid analogs were purchased from Iris Biotech or Bachem. PepChem provided the trityl chloride polystyrene resin. The chelators DOTAGA (2-(4,7,10-tris(carboxymethyl)-1,4,7,10-tetraazacyclododecan-1-yl)pentanedioic acid), DOTA (1,4,7,10-tetraazacyclododecane-1,4,7,10-tetraacetic acid), NOTA and their derivativeswere supplied by Chematech. Alfa Aesar, Sigma-Aldrich, Fluorochem or VWR provided the solvents and organic reagents.

The tBu-protected PSMA binding motifs Glu-urea-Glu ((tBuO)EuE(OtBu)2) and Lys-urea-Glu ((tBuO)KuE(OtBu)2) and the derivative PfpO-sub-(tBuO)KuE(OtBu)2 (pentafluorophenylic acid-active ester of the tBu-protected EuK binding motif) were prepared analogously to known procedures. The synthesis of the silicon fluoride acceptor 4-(di-tert-butylfluorosilyl)benzoic acid (SiFA-BA) and the alkyne-functionalized TRAP chelator (1,4,7-triazacyclononane-1,4,7-tris[methyl(2-carboxyethyl)phosphinic acid) was performed according to appropriate protocols.

Solid phase synthesis of peptides was performed manually using a syringe shaker (Intelli, Neolab). Shimadzu gradient systems (Shimadzu) were used for

analytical and preparative HPLC, each equipped with an SPD-20A UV/Vis detector (220 nm, 254 nm). Analytical measurements were performed with a Nucleosil 100 C18 (125 × 4.6 mm, 5 µm particle size) column (CS Chromatography Service) at a flow rate of 1 mL/min. at a constant flow rate of 5 mL/min, preparative HPLC purification was performed with a Multospher 100 RP 18 (250 × 10 mm, 5 µm particle size) column (CS Chromatography Service). Analytical and preparative radio HPLC was performed using a Nucleosil 100 C18 (5 µm, 125 × 4.0 mm) column (CS Chromatography Service). The eluants for the HPLC operations were water (solvent A) and acetonitrile (solvent B), both containing 0.1% trifluoroacetic acid. Radioactivity was detected by connecting the output of the UV photometer to a HERM LB 500 NaI detector (Berthold Technologies). Electrospray ionization mass spectra for characterization of the compounds were recorded using an expression LCMS mass spectrometer (Advion, Harlow). Bruker (Billerica, USA) AVHD-300 or AVHD-400 spectrometers at 300 K were used to record nuclear magnetic resonance spectra. A 2480 WIZARD2 automatic gamma counter (PerkinElmer) was used for activity quantification. A scanning RAM detector (LabLogic Systems) was used to perform radio-thin-layer chromatography.(Wurzer et al., 2020)

3.1.2 Manual 18F labeling

Klinikum rechts der Isar provided 18F-fluoride (~0.6-2.0 GBq/mL). For manual 18F labeling, aqueous 18F- was passed through a strong anion exchange cartridge (Sep-Pak Accell Plus QMA Carbonate Plus Light cartridge, 46 mg, 40 µm; Waters) preconditioned with 10 mL of water. Most of the remaining water

was removed with 20 mL of air, and any residue was removed by rinsing the cartridge with 10 mL of anhydrous acetonitrile (for DNA synthesis, VWR) followed by 20 mL of air. For cartridge elution, [K+⊂2.2.2]OH kits containing a lyophilized mixture of 2.2.2-cryptand (Kryptofix 222, 110 µmol, 1.1 equivalent, Sigma Aldrich) and KOH (100 µmol, 1.0 equivalent, 99.99% semiconductor grade, Sigma Aldrich) dissolved in 500 µl of anhydrous acetonitrile before the elution process were used. The eluate was then partially neutralized with 30 µmol oxalic acid (99.999%, trace metal grade, Sigma Aldrich) in anhydrous acetonitrile (1 M, 30 µL). The resulting mixture was used as a whole or aliquot for fluorination of 10-150 nmol of an appropriate labeling precursor (1 mM) in anhydrous dimethyl sulfoxide (>99.9%, Sigma Aldrich) for 5 min at r.t.. An Oasis HLB Plus Light cartridge (30 mg sorbent, 30 µm particle size; Waters), preconditioned with 10 mL water, was used to purify the tracer. The labeling mixture was diluted with 9 mL phosphate-buffered saline (PBS, pH 3, adjusted with 1 M aqueous HCl) and passed through the cartridge, followed by 10 mL PBS (pH 3) and 10 mL air. The peptide was eluted with 0.3-2.0 mL of a 1:1 mixture (v/v) of ethanol in water. The RCP of the 18F-labeled compound was determined by radio-thin layer chromatography (silica gel 60 RP-18F254s, mobile phase: 3: 2 mixture (v/v) of acetonitrile in water supplemented with 10% 2-M sodium acetate solution and 1% trifluoroacetic acid) and radio-RP HPLC (Nucleosil 100 C18, 5 µm, 125 × 4.0 mm, mobile phases water and acetonitrile, both with 0.1% trifluoroacetic acid.(Wurzer et al., 2020)

3.2 Patients

Between June 2017 and March 2018 patients with BCR after RP underwent clinicaly indicated 18F rhPSMA-7-PET/CT at the department of Nuclear Medicine at Klinikum rechts der Isar and their data was reviewed retrospectively. All patients had undergone a curatively intended RP or salvage RP after EBRT. Prior details of the patients with regard to PSA-nadir and PSA-kinetics were documented as well as the actual PSA-levels prior to PET/CT.

Castrate resistent PC patients were excluded. Contraindications for CT or MRI like renal impairment, implants or devices and the presence of metallic foreign bodies excluded patients from the study. Further reasons for exclusion of the study were known hypersensitivity to any of the ingredients of the used radiohybridpharmacon or contrast like iodine or known hyperthyroidism. Further exclusion criteria were claustrophobia, previous experimental therapy with other PSMA-ligands or other investigational therapies, including cryotherapy, high intensity focused ultrasound (HIFU) as well as focal therapy.

All patients gave written informed consent for the procedure. All investigations were conducted with national regulations and in accordance with the Helsinki Declaration. The local Ethics Committee (permit 290/18S) approved the retrospective analysis. The administration of 18F-rhPSMA-7 complied with the German Medicinal Products Act, AMG §13 2b, and the responsible regulatory body (government of Oberbayern).

3.3 18F rhPSMA-7 administration and imaging

Patients were given 20 mg furosemide i.v. 20 min prior to the scan to reduce tracer accumulation in the urinary tract and thus to prevent poor image quality.

After informed consent, an 18G or 20G indwelling vein cannula was injected into an arm vein and the 18F rhPSMA-7 solution was injected, followed by 10ml saline. The applied amount of tracer was determined before and after measurement of the activity with an activimeter and these time points were documented.

At a median of 76 min (mean, 82 ± 22 min; range, 50-220 min) prior to scanning an intravenous bolus was administered with a median activity of 332 MBq -18F-rhPSMA-7 (mean, 330 ± 34 MBq; range, 143-486 MBq).

All examinations were carried out in the same way and according to the hospital's internal SOP. Imaging was performed in a standardized supine position with the arms crossed over the head with a Biograph mCT flow scanner (Siemens Medical Solutions, Erlangen) at the Department of Nuclear Medicine at the Klinikum rechts der Isar of the Technical University of Munich. A diagnostic CT scan was performed in the portal venous phase 80 seconds after intravenous injection of the contrast agent (Iomeron 300), followed by the PET scan. The patients received the diluted oral contrast medium (300 mg of ioxitalamate [Telebrix; Guerbet]). PET scans were acquired in 3-dimensional mode with an acquisition time of 1.1 mm/s. Emission data were corrected for scatter and attenuation, randomization and dead time and iteratively reconstructed using an expectation maximization algorithm for ordered subsets (4 iterations, 8 subsets), then gaussian filtered after reconstruction (5 mm full width at half maximum).

There were no examination-related side effects.

3.4 Data analysis and evaluation of the images

Images were reviewed by an experienced board-certified nuclear medicine physician and a board-certified radiologist.

Imaging analysis was done by acknowledged radiological and nuclearmedicine known criteria. Imaging analysis took place at Syngo Via (Siemens Medical Solutions, Erlangen) workstation.

All BCR suspicious lesions were noted. Any focal tracer uptake that was not accompanied by physiologic uptake due to tumerous sclerotic leasons or was higher than the surrounding background was considered a possible malignancy. Low to moderate PSMA expression due to osteoblastic changes, for example, fractures or degenerative changes, as well as low uptake associated with celiac and other ganglia, were reported as typical pitfalls of PSMA ligand PET imaging (Hofman, Hicks, et al., 2018).

All suspicious lesions were noted and categorized as local recurrence in the prostate bed, lymph node metastases, extensively stratified by location as pelvic, retroperitoneal, or supradiaphragmatic metastases, and bone metastases or other metastases in distant organs such as lung or liver.

3.5 Determination of Data

The following patient data were collected using Microsoft Excel spreadsheet (Microsoft Office 2010, Microsoft Corporation, Redmond, USA) on a password-protected institutional computer.

- patient data including name, surname, address, phone number (these were later anonymised), date of birth, and age at day of imaging as well as imaging date

- disease relevant data like date of primary illnes, initial PSA-level, GS of punch-biopsy, BCR after RP including salvage RTx when PSA was greater than 2ng/ml, BCR after EBRT (RTx) and PSA greater than 2ng/mL, primary therapy (RTx, CTx, Brachytherapy, ADT), PSA-Nadir, histology of the resected prostate (T-,N- status after TNM classification, number of resected and positive lymphnodes, R-status and GS)
- ADT in the last 6 month prior to imaging (yes/no), at least two PSA-values before imaging and change of therapy (yes/no)
- modality of imaging (PET/CT or -MRI)
- variables of the 18F-rhPSMA-7 imaging including most recent PSA-value, patient weight, time of and injected MBq activity, time between tracer injection and imaging in minutes and localisation of tumor suspicious sides (local recurrence, pelvic, retroperitoneal, supradiaphragmatic lymph node metastases, bone metastases and visceral metastases)
- follow-up-parameters including further procedures like salvage surgery including histology and type of surgery (secundary lymphadenectomy or PSMA-radioguided surgery), salvage-RTx, ADT, palliative or ‘wait-and-see’ approach

3.6 Procedure for data acquisition

Data collection was obtained through targeted research from hospital records, which consisted of patient records, doctor's letters from the urology department and nuclear medicine, radiotherapy, nursing-, surgery-, anaesthesia- and pathology-reports, as well as laboratory findings. The documentation systems

included SAP (Walldorf, Germany) and the PACS (picture archiving and communication system) of Klinikum rechts der Isar.

3.7 Statistical analysis

The detection rate of suspicious recurrence sites was plotted against baseline PSA. Both for recurrence, in terms of the number of patients, with at least one positive finding and in terms of regional local recurrence, lymph node metastases, bone metastases, and other distant metastases. Patient-level detection rates were correlated with primary GS, prior ADT, and EBRT.

Statistical analyses were performed using MedCalc software (version 13.2.0). Two-sample t-tests were used to evaluate differences between groups (GS, ADT), and Mann-Whitney U tests were used to evaluate differences in PSA levels between groups with and without pathologic uptake. All tests used a significance level of $\alpha = 5\%$ and were two-sided.

- the PSA value was evaluated as a continuous variable in five subgroups <0.2, 0.2-<0.5, 0.5-<1, 1-<2, ≥2 ng/mL
- the GS was evaluated as a continuous variable and in the two categories ≤7 and ≥8
- patient age is coded as a continuous variable
- ADT within the last 6 months before imaging (yes/no) is a categorical variable, as is the modality of imaging (PET/CT or.-MRI)

3.8 Data protection

The data was treated confidentially in accordance with medical confidentiality. The data was processed exclusively on the clinic's own computers without network access and exclusively by authorised personnel. All Helsinki guidelines and the guidelines of the ethics committee as well as the guidelines of data protection were fulfilled.

4.Results

A collective of 532 patients were included in the study with a median age of 71 years and a median pre-scan PSA-level: 0.97 ng/mL (0.01- 372ng/mL).

123 (23.2%) patients had a ADT in the six month prior imaging.

225 (42.3%) patients underwent EBRT after RP. 423 of the 532 patients (79.5%) showed one or more localized areas suggestive of recurrent prostate cancer. Further patient information see Table 1.

4.1.1 Clinical and pathologic characteristics

- Table 1

Age (years)	71	(48-89)
Further treatment		
• EBRT	225	(42.3%)
• HTx	168	(31.6%)
• ADT 6 month prior Pet scan	123	(23.1%)
Gleason Score		
• ≤ 6	24	(4.5%)
• 7	208	(38.1%)
• ≥ 8	173	(32.5%)
• unknown	127	(21.6%)
Pathologigal primary tumor staging at RP		
• pT2	152	(28.6%)
• pT3	288	(54.1%)
• unknown	92	(17.3%)
Pathological regional lymph node staging at RP		
• pN0	296	(55.6%)
• pN1	118	(22.2%)
• pNx	118	(22.2%)
Positive margin at RP		
• R0	206	(28.7%)
• R1	143	(26.9%)
• Unknown	183	(34.4%)
Median initial PSA-value (ng/mL)	10	(0.02-290)
Median time between surgery and Pet (month)	56	(0-336)
Last median PSA-value before Pet (ng/mL)	0,97	(0- 400)
Median injected activity (MBq)	332	(143-486)
Median uptake time (min)	76	(50-220)

4.1.2 Detection rate stratified by PSA-value

- Table 2

PSA-value in ng/mL	No. positive/all	%
<0.2	15/39	38.5
0.2 - <0.5	81/127	63.8
0.5 - <1	90/104	86.5
1 - <2	87/102	85.3
≥2	150/160	93.8
overall	423/532	79.5

- Figure 5

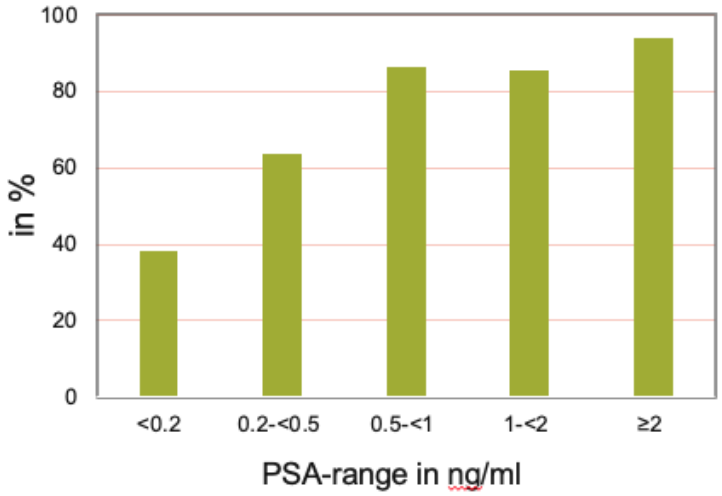

The detection efficacy of 18F-rhPSMA-7 PET/CT is correlated positively with PSA levels and was 93.8% (150/160; 95% confidence interval [CI], 0.89–0.97) for a PSA value of ≥2 ng/mL, 85.3% (87/102; 95% CI, 0.77–0.92) for a PSA value of 1 to 2 ng/mL, 86.5% (90/104; 95% CI, 0.78–0.92) for a PSA value of 0.5 to 1 ng/mL, 63.8% (81/127; 95% CI, 0.55–0.72) for a PSA value of 0.2 to 0.5 ng/mL, and 38.5% (15/39; 95% CI, 0.23–0.55) for a PSA value of <0.2 ng/mL (Tab.2, Fig.3). The mean and median PSA level was significantly lower

among patients with negative results on 18F-rhPSMA-7 PET/CT than among those with positive results (Tab.3).

4.1.3 PSA Level in Patients with Positive Vs. Negative 18F-rhPSMA-7 PET/CT Results

- Table 3

	PSA, mean ± SD /median (ng/mL)		
	positive findings	no findings	p
PSA-level mean(ng/mL)	5.79± 28.1	0.86± 1.6	<0.001
PSA-level median(ng/mL)	1,18± 7,46	0,4± 0,84	<0.001

18F-rhPSMA-7–avid lesions were detected in prostatic and extra prostatic regions as shown in Table 4 and Figure 4. Regional positivity also increased with increasing PSA level. Local recurrence in the prostate bed ranged from 18% at PSA 0.2 ng/mL to 48% at PSA 0.5- <1.0 ng/mL, whereas pelvic lymph node metastases were present in 18% at PSA <0.2 ng/mL to 63% at PSA ≥2 ng/mL. Although retroperitoneal lymph node metastases were rare at lower PSA levels, 3% at 0.2 ng/mL, 36% of patients with PSA ≥2 ng/mL had positive retroperitoneal lymph nodes, respectively. Distant lymph node metastases were rare in very early BCR, with no supradiaphragmatic lymph node metastases observed at PSA <0.2 ng/mL. However, 16% of patients with PSA ≥2 ng/mL were found to have positive supradiaphragmatic lymph nodes. 18F-rhPSMA-7–avid bone lesions were present early in 18% of patients with PSA <0.2 ng/mL and 37% of patients with PSA ≥2 ng/mL. Visceral metastases were absent or low across all PSA levels. There were no visceral metastases detected for a PSA <0.2 ng/mL, 0.8%, 3.8% and 2% for PSA levels of 0.2- <0.5

ng/mL, 0.5- <1.0 ng/mL and 1-2 ng/mL, respectively. Only 9% of patients with PSA ≥2 ng/mL were found to have visceral metastases (Table 4 and Figure 4).

4.1.4. Distribution of 18F-rhPSMA-7–Avid Lesions Stratified by PSA Value

- Table 4

PSA-value (ng/mL)	Local recurrence	Pelvic lymph nodes	Retroperitoneal lymph nodes	Supradiaphragmatic lymph nodes	Bone metastases	Visceral metastases
<0.2	7/39 (17.9%)	7/39 (17.9%)	1/39 (2.6%)	0/39 (0.0%)	7/39 (17.9%)	0/39 (0.0%)
0.2- <0.5	45/127 (42.5%)	25/127 (19.7%)	7/127 (5.5%)	1/127 (0.8%)	12/127 (9.4%)	1/127 (0.8%)
0.5- <1.0	50/104 (48.1%)	39/104 (37.5%)	7/104 (6.7%)	3/104 (2.9%)	17/104 (16.3%)	4/104 (3.8%)
1-2	43/102 (42.2%)	48/102 (47.%)	16/102 (15.7%)	7/102 (6.9%)	17/102 (16.7%)	2/102 (2.0%)
≥2	70/160 (43.8%)	101/160 (63.1%)	57/160 (35.6%)	25/160 (15.6%)	59/160 (36.9%)	14/160 (8.8%)

- Figure 4

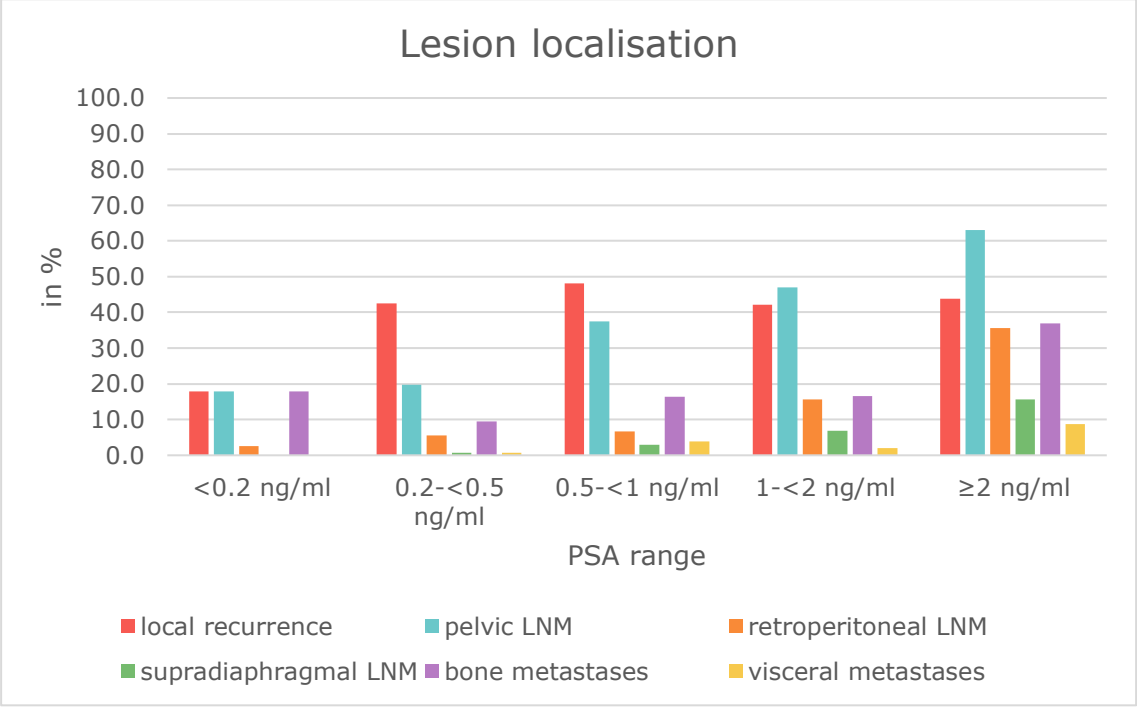

4.1.5 Influence of Prior Therapy and Primary Histologic Differentiation

We observed no significant difference between the detection rate among patients who had previously received EBRT (77.5% (238/307)) and those who had not (82.2% (185/225), P 0.185). Receiving ADT in the six months prior to the scan also did not appear to affect the results (84.6% (104/123) compared with 78.0% (319/409) for no prior ADT, (P 0.114). When considering the histologic differentiation at the primary diagnosis, 18F-rhPSMA-7 PET/CT was positive in 77.2% (179/232) of patients with a Gleason score of 7 or less and in 85.0% (147/173) of patients with a Gleason score of at least 8 (P 0,001). Therefor a significant difference showed regarding primary histological differentiation (Table 5).

4.1.5 Detection rate stratified by EBRT, ADT within six-month prior imaging and primary GS

- Table 5

	Detection efficacy in % (No. +/all)		
	yes	**no**	**P**
Prior EBRT	82.2 (185/225)	77.5 (238/307)	0.185
ADT within 6 months prior imaging	84.6 (104/123)	78.0 (319/409)	0.114
Primary histological differentiation	**GS ≤7*** 77.2 (179/232)	**GS ≥8*** 85.0 (147/173)	<0.001

Note: * primary histological differentiation not known in all patients

4.5 Comparable diagnostic value to 68GA-PSMA-11 and other 18F-PSMA-Tracers according to the literature

- Figure 5

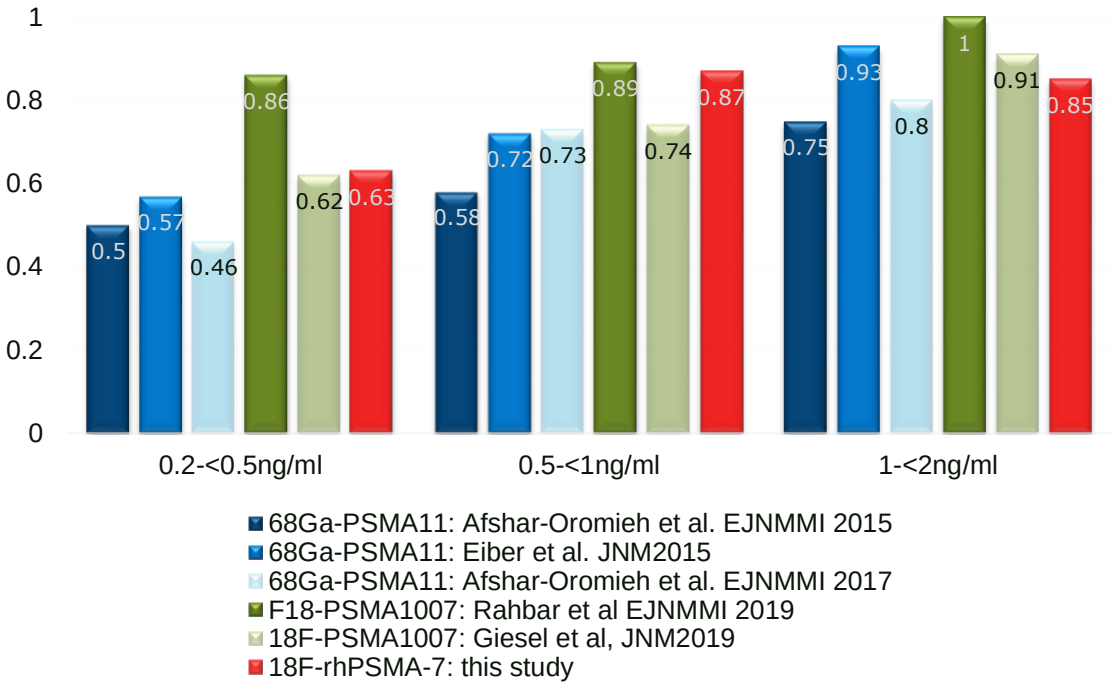

Note: The 18F-rhPSMA-7-Tracer shows comparable results for diagnoctic value as commonly used 68Ga-PSMA-Tracers. Its advantage lies at higher detection rates in the cohorts with lower PSA-values 0.2-1ng/ml.

- Figure 6

Patient example

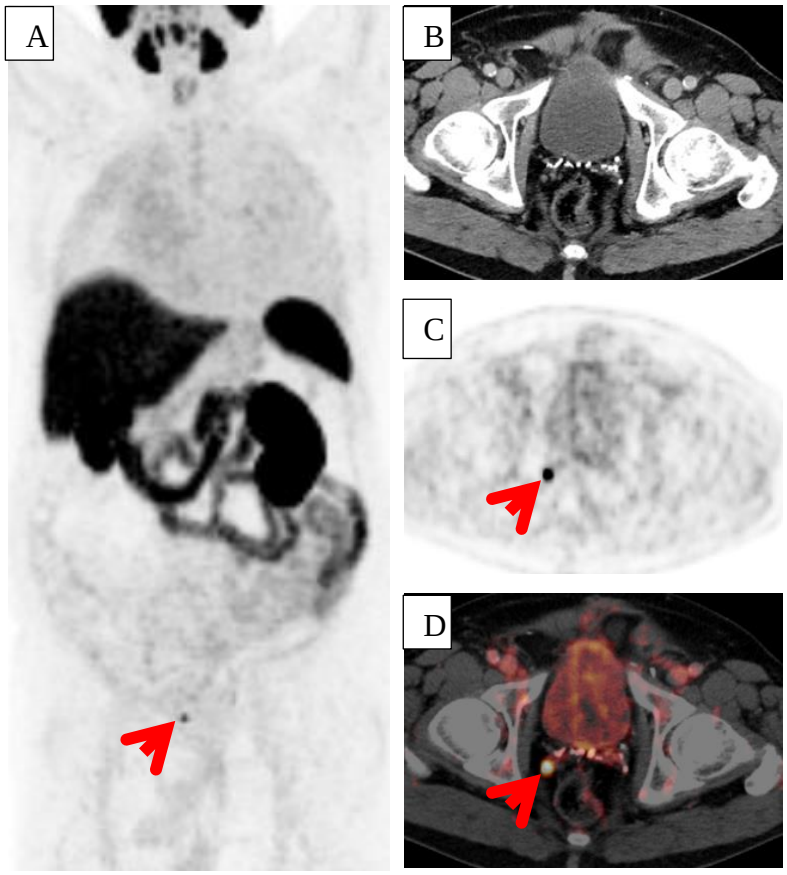

Note: Image from 78-y-old patient who underwent radical prostatectomy (Gleason score of 8, pT3a, pN0) and was experiencing rising PSA (0.35 ng/mL). A) Whole-body maximum-intensity projection shows one site with focal PSMA-ligand uptake in pelvis (arrow). Axial fused PET/CT (C) demonstrate local recurrence. The local tumor is not detectable on CT (B) but shows increased tracer uptake on 18F-rhPSMA-7 PET and PET/CT (D). A small lymph node ventral to right external iliac vein; corresponding 18F-rhPSMA-7 PET and PET/CT images show an intense uptake with high lesion-to-background ratio in this small lymph node, indicating a lymph node metastasis. Targeted external-beam radiation treatment led to subsequent PSA drop.

5. Discussion

Very early detection of recurrence is of utmost clinical importance to plan the individual salvage therapy approach, as it offers the best chance of cure for patients with BCR after prostatectomy (Emmett et al., 2017; Mottet et al., 2017; Sterzing et al., 2016). Before the patient's PSA level reaches 0.5 ng/mL, more than 60% of patients achieve an undetectable PSA level with salvage radiotherapy, and the chance of being progression-free after five years increases to 80% (Fossati et al., 2016; Pfister et al., 2014; Sargos et al., 2020; Stish et al., 2016; Wiegel et al., 2009). To detect recurrent foci at an early stage of recurrence, different PET agents have a clinical benefit that influences a patient's future treatment (Andriole et al., 2019; Goldstein et al., 2017; Perera et al., 2020; Van den Broeck et al., 2019). The detection of lymph nodes and distant metastases, as well as the detection of positive surgical margins (PSMs) has the greatest impact on patient secondary treatment and palliative radiotherapy (Han et al., 2018; Kvåle et al., 2019). Rising PSA levels after RP usually precedes a clinically detectable recurrence by years (Van den Broeck et al., 2019). As mentioned above, currently a PSA level of greater than 0.2 ng/mL is the definition of BCR of prostate cancer after RP (Mottet et al., 2011). Still, it cannot differentiate between local, regional, or systemic disease recurrence. Therefore, precise imaging techniques are required to identify areas of involvement to then deliver an optimized therapy.

Conventional imaging techniques, such as ^{11}C-choline PET, are very limited in patients with low PSA values and are not recommended for those with a PSA level of below 1 ng/mL (Castellucci et al., 2009; Mottet et al., 2017). Giovacchini et. al. only showed detection rates of 7.8-28.1% for choline-based tracers for

PSA-values of 0.2 and 0.5ng/ml, respectively. PSMA-targeting agents have shown to be more efficient in determining the sites of disease and have had a major impact on patient management (Henninger et al., 2016; Perera et al., 2016). Although 68Ga-PSMA-11 PET is in increasing use in research studies, where it has shown encouraging results, it has not been currently approved by the European Medicines Agency or the U.S. Food and Drug Administration.

This study investigated a large, homologous patient cohort with biochemical recurrence after radical prostatectomy, who underwent imaging with the novel 18F-rhPSMA-7-tracer. It has shown to be highly effective in restaging of this cohort, with the site of disease recurrence showing in 76 % of all patients and in 94% of those with a PSA level of 2 ng/mL or greater.

Perera et.al. presented a large meta-analysis about 68Ga-PSMA-PET in advanced prostate cancer, for PSA categories 0–0.19, 0.2–0.49, 0.5–0.99, 1–1.99, and >2 ng/ml, where the percentages of positive scans were 33%, 46%, 57%, 82%, and 97%, respectively compared to 38.5%, 64%, 87%, 85% , 94% for a PSA value of <0.2 ng/mL, 0.2 to 0.5 ng/mL, 0.5 to 1 ng/mL, 1 to 2 ng/mL and ≥2 ng/mL, with 18F-rhPSMA-7 respectively. Thus, the high detection rates of 18F rhPSMA-7 diagnostics were confirmed in the present study even though our median pre-scan PSA-level with 0.97 ng/mL was lower than most studies included by Perera et. al.(Perera et al., 2020). The detection rate for 18F-rhPSMA-7 in this study increases with increasing PSA value**,** consistent with the results of other PET-tracers. For example the recent 18F-PSMA-1007 showed detection rates 94.0% (79/84), 90.9% (50/55), 74.5% (35/47), and 61.5% (40/65) for PSA levels of greater than or equal to 2, 1 to less than 2, 0.5

to less than 1, and 0.2 to less than 0.5 ng/mL, respectively (Afshar-Oromieh et al., 2017; Giesel et al., 2019; Maurer, Gschwend, et al., 2016).

This previous data suggests that, especially at low PSA values, 18F-labelled PSMA tracers can lead to higher detection rates than reported for 68Ga-labelled PSMA tracers. Present data supports this, notably for PSA levels of less than 0.5 ng/mL (Giesel et al., 2019; Maurer, Gschwend, et al., 2016). Dietlein et.al also confirmed this especially for low PSA levels around 0.45 µg/L, where local sensitivity of 18F-DCFPyL reached 62%, whereas 68Ga-PSMA-HBED-CC only detected disease recurrence in 33% of the patients (Dietlein et al., 2017). Although the detection rates drop with a lower PSA value, the salvage therapy must not be delayed. A low PSA value might represent a low tumor volume and therefore a low PSMA expression with little tracer uptake, but the tumor might still be aggressive (Mottet et al., 2011).

The different energy profiles of 18F and 68Ga may be accountable for superior detection rates of 18F. The shorter half-life and lower positron yield of 68Ga compared to 18F is a limiting factor and detection sensitivity for 68Ga was found to be up to 15% lower than for 18F. Image noise in 68Ga based PET imaging also is slightly increased due to single photon emission in a low energy range and scattered photons falling in that acquisition energy window. Theoretically, the achievable resolution of 18F is higher than that of 68Ga (Giesel et al., 2018) (Sanchez-Crespo, 2013). Tumor to background noise makes clearer imaging possible and recognition of smaller lesions easier.

Additionally, the described low urinary retention of 18F-rhPSMA- 7 at one hour after injection might have a favourable effect on the enhanced detection efficacy

(Wurzer et al., 2020). High accumulation of 68Ga-PSMA-11 in the bladder during imaging impairs the detection of small local recurrences, especially when in close proximity to the bladder (Freitag et al., 2016). In a recent study of 68Ga-PSMA-11-imaging in a large cohort of 272 patients, local recurrence was detected in 20% and 30% at PSA levels of 0.2-0.5 and 0.5-1.0 ng/mL, respectively [77], compared with 43% and 48%, respectively, in the present study (Table 4). The results may have been influenced by differences in patient cohorts such as those based on different examination protocols. The timing of imaging after tracer application, the use of furosemide, or permanent bladder catheterization during imaging may reduce retention of 68Ga-PSMA-11 in the bladder [75]. Therefore, comparison with the literature remains a challenge.

However, it must be said that this study has not yet performed a systematic histological control of PSMA-positive PC foci. Thus, sensitivity and specificity of this study can hardly be assessed and only a general detection rate compared to conventional imaging can be estimated and related. Nevertheless, reference should be made here to the study by Kroenke et. al., which support the hoped-for results of the investigated tracer and thus also make it considerable for recurrence diagnostics. In their study, Kroenke at. al. compared the images with histopathology. Sensitivity was 72.2% (95% CI, 46.5%–90.3%) and specificity, 92.5% (95% CI, 79.6%–98.4%). In total, 18F-rhPSMA-7 PET showed an accuracy of 86.2% (95% CI, 74.6%–93.9%) on patient-based analysis (Kroenke et al., 2019).

Although this cohort studied was highly homologous, the effects of primary histologic classification (GS) and prior treatment on the detection rate for 18F-rhPSMA-7 were examined.

In our patient cohort, the detection rate for 18F-rhPSMA-7 showed a significant difference between the GS≤7 and GS ≥8 groups, 77.2% (179/232) vs. 85% (147/173), P <0,001, respectively. Perera et. al. published meta-analysis which included ten studies and 1651 patients provided data on the positivity of 68Ga-PSMA PET based on biopsy or prostatectomy histopathology GS. The meta-analysis found no significant difference between 68Ga PSMA PET positivity and GS. Patients with a GS of 7 had a positivity of 72% vs. 80% in patients with a Gleason sum of 8 (p > 0.30). Older studies from Afshar-Oromieh et al. and Verburg et al. both didn't show significance regarding a higher GS and positive imaging.

Data suggest that overexpression of PSMA increases with GS, even though these reports mainly focus on the GS of the primary tumor (Chu et al., 2021; Karyagar et al., 2020; Ross et al., 2003). Indeed, a cohort of patients with BCR could already represent a selection of more aggressive phenotypes of prostate cancer and support the actual data. However, this finding loses some of its significance when considered that the evaluation of GS is entirely dependent on the expertise of the pathologist and can be either overestimated or underestimated (Bravaccini et al., 2018).

123 (23%) of our patients underwent ADT within the last six months prior to the study. Several preclinical studies have reported on the effect of ADT on PSMA expression, however, most of these studies used conventional PC cell lines, which do not have the genetic diversity of PC patients. Many of these preclinical

studies reported an increase in PSMA-levels after ADT (Hope et al., 2017; Roy et al., 2021). Overall, clinical studies showed that the type of PC and duration of ADT may have a differential impact on PSMA levels (Aggarwal et al., 2018; Emmett et al., 2019; Hope et al., 2017; Leitsmann et al., 2019; Meller et al., 2015; Onal et al., 2020; Wright et al., 1996). Short-term ADT therapy resulted in the increase of PSMA-expression and a decrease was observed with long-term ADT (Afshar-Oromieh et al., 2018; Ettala et al., 2020). One study even demonstrated an increased number of lesions showing at imaging after one month of ADT treatment although the PSA levels had decreased (Hope et al., 2017). The molecular mechanisms that modulate these heterogeneous PSMA responses to ADT remain to be elucidated and may potentially provide clinically relevant information on the use of PSMA-targeted therapeutics with or without ADT. For example, patients who have elevated PSMA levels after ADT may benefit from combination therapy including a PSMA-targeted therapeutic agent such as [177Lu]PSMA-617 (Giesel et al., 2016; Hofman et al., 2019; Wurzer et al., 2020). In contrast, patients with low levels of PSMA after ADT are most unlikely to benefit from additional PSMA-targeted therapies (Hofman, Violet, et al., 2018). It should be noted that patients who have already received ADT are likely to have more advanced disease than patients who have not received ADT. This may be a confounding factor for these data in the literature. The role of ADT in the uptake of PSMA-based tracers is highly controversial as ADT appears to increase PSMA expression at the cellular level, but the treatment may also lead to a reduction in tumor cells. This represents an opposing effect (Hope et al., 2017). Nevertheless, as in previous studies with 68Ga-PSMA-11, no significant influence on the detection rate with 18F-rhPSMA-7 could be detected using ADT within the last 6 months prior to the study (Eiber et al.,

2015). Together with their treating physicians' patients with a PSA increase decide, whether they should receive ADT in the near future. There is no standard recommendation in the guidelines (Van den Broeck et al., 2020).

The aim of this study was to detect BCR after RP for the first time with 18F-rh-PSMA-PET, but previous negative imaging was not a criterion for exclusion, resulting in a possible selection bias that must be considered. However, a positive correlation between the time of ADT prior to and PSMA-mediated imaging could open new possibilities for PSMA diagnostics (Hope et al., 2017). This needs to be further investigated. In this study we only differentiated between ADT yes or no within prior six month of the 18F-rh-PSMA imaging. Data regarding duration, exact indication, type of medication and dosage could not be collected and therefore the comparability with other studies is very limited.

PSMA ligand uptake in degenerative changes**,** healing fractures, or fibrocartilage lesions has been described previously, as with the recently published data for 18F-PSMA1007 (Hofman, Hicks, et al., 2018; Hövels et al., 2008; Jochumsen et al., 2018; Sheikhbahaei et al., 2017). PSMA ligand uptake into bone was observed. This may be due in part to such nonspecific uptake. CT plays an important role in this case. Jannsen et. al. found out that by adding low dose CT information, a significant reduction in equivocal lesions was achieved for both 68Ga-PSMA-PET and SPECT for detecting bone metastasis (Janssen et al., 2018). Appropriate findings are essential for a correct differential diagnosis. There are no specific features of PC bone metastases, however, PSMA avidity tends to be higher in the evaluation of malignant bone

lesions than benign pathologies, which usually have low to moderate uptake (Barbosa et al., 2019).

When evaluating a bone lesion, the morphologic aspects on CT, such as the number of lesions, the type of margin, the pattern of bone destruction, the type of periosteal reaction, and the presence of an associated soft tissue mass, needs to be considered. Benign appearances often show slow-growing lesions with sharply demarcated margins, geographic destruction, and smooth, uninterrupted periosteal reaction without a soft tissue mass.

As osteodegenerative changes are very common in PC patients and with exceptional PSMA uptake, the typical morphologic appearance of joint space narrowing with sclerosis and osteophytosis is a clue to the diagnosis (Janssen et al., 2018).

The high variability of morphologic imaging by CT and MRI is a problem in clinical diagnostic performance for lymph node metastases (Hövels et al., 2008). Up to 80% of metastatic lymph nodes are normal in size and thus <8mm. Therefore, characterization of lymph nodes by size alone is of limited utility because, as known from 68Ga-PSMA-11, lesion size is critical for their detection (Jilg et al., 2017). Evaluation of data on detection efficacy using 18F-rhPSMA-7 was studied by Kroenke et.al. That retrospective analysis showed that PET with 18F-rhPSMA-7 has high diagnostic accuracy **for N-staging** in patients with primary high-risk PC. The efficacy is superior to that of morphologic imaging, which is recommended in most guidelines (Kroenke et al., 2019; Mottet et al., 2017). Kroenke et. al presented data, where the mean size of negative lymph node templates was similar to that reported by Maurer et al (3.5 mm) (Maurer, Gschwend, et al., 2016). It shows that PSMA ligand

tracers provide a favourable lesion-to-background ratio for detecting metastatic lymph nodes because PSMA is not expressed by normal lymphoid or retroperitoneal fatty tissue. With common morphologic imaging, sensitivity decreased to 9.6% (95% CI, 4.5%-19.3%). The accuracy of 18F-rhPSMA-7-PET was 86% and 91%, respectively, compared with 66% and 83% for morphological imaging and performance of 18F-rhPSMA-7 seems comparable with 68Ga-PSMA-11. The potential to detect organ (e.g.bone) metastases was not investigated in their analysis (Kroenke et al., 2019).

Comparisons with other 18F-labelled PSMA ligands is limited due to the lack of published data. But Gorin et al. reported data from a small prospective study with 18F-DCFPyl including 25 patients. Here, sensitivity and specificity were 71.4% (95% CI, 29.0-96.3) and 88.9% (95% CI, 65.3-98.6), respectively (Gorin et al., 2018). In their study, 98.3% of patients (57/58) had high 18F-rhPSMA-7 uptake in the local tumor (Kroenke et al., 2019). Giesel et al. demonstrated an excellent overall sensitivity for pelvic lymph node metastases of 94.7% for 18F-PSMA-1007 PET/CT with lesions detected as small as 1mm in diameter and thus very promising for early detection of BCR (Giesel et al., 2017).

Radical prostatectomy was an average of 72.75 months prior to imaging (0-336 months, median 56 months). As in previous studies, there was no significant correlation between latency and detection rate.

The available data showed local recurrence in 42.1% (224/308) of PSMA-positive patients. Of these, 64 (12%) patients had a PSA value below 0.5 ng/mL. 93 (17.5%) had a PSA value of 0.5-1.0 ng/mL and 70 (13.15%) of patients had a PSA value >2.0ng/mL. Regarding 68Ga-PSMA-PET imaging Perera et al found 22% in local recurrence among those who underwent

prostatectomy (Perera et al., 2020). Which is quite low compared to this study. The estimates of positivity in all screening studies were 38% in pelvic lymph nodes, 22% in bone, and 5% in distant viscera, for the 13 studies including BCR after RP, resembling mostly our results (Perera et al., 2020). Extra-pelvic lesions seemed to be better detected by 68Ga-PSMA-PET with a detection rate of 13%. In this study only 6,8% for 18F-rh-PSMA7-Pet were detected. Similar results were obtained in a study comparing 68Ga- and 18F-tracers. Lesions attributed to recurrent PC on 68Ga-PSMA-11 PET compared with 18F-PSMA-1007 PET were as follows: abdominopelvic lymph nodes in 34% and 29%, local recurrence in 26% and 22%, supradiaphragmatic lymph nodes in 17% and 27%, bone metastases in 21% and 18%, and other soft tissue metastases in 2% and 4%, respectively. Local recurrences detected by 18F-PSMA-1007-PET were more frequently located directly adjacent to the urinary bladder (59.3%), than local recurrences detected by 68Ga-PSMA-11-PET (48.5%). In addition, local recurrences identified by PSMA ligand imaging but not directly adjacent to the urinary bladder were closer to the bladder wall on 18F-PSMA-1007-PET than on 68Ga-PSMA-11-PET. This may argue for a better tumor to background ratio (Rauscher et al., 2020). Two other recent studies from Giesel et. al. and Rahbar et. al. about the 18F-PSMA-1007 tracer showed an overall better performance compared to 68Ga. (Figure 10) (Giesel et al., 2019; Rahbar, Afshar-Oromieh, et al., 2018) Thus, there may be an advantage in the performance of 18F-labeled tracers over the commonly used 68Ga. Since Perera's meta-analysis also included patients with previous RTX and the present study only includes patients after RP, this might influence different results. The different imaging modalities of PET/MRI and PET/CT may also have contributed to such differences. Although previous studies found no

significant difference in detection rate between the two imaging modalities, there were advantages in the functional diffusion-weighted imaging of MRI, which might be of interest when PET/CT images are unclear (Freitag et al., 2016). In a recent study from Chen et. al. no difference was observed between PET/CT and PET/MRI both on extracapsular extension and seminal vesicle invasion diagnosis (Chen et al., 2020). Nevertheless, MRI will probably never replace CT because of economic reasons, as PET/MRI remains expensive and unavailable for routine use. Also, the fact that most patients with prostate cancer are of older age and therefore the radiation-related long-term effects do not play a major role.

The novel PSMA ligand 18F-rhPSMA-7 offers several advantages over more established PSMA-based tracers such as 68Ga-PSMA-11 and has already shown encouraging data for the detectability of BCR (40). 18F-rhPSMA-7 shows a great logistical advantage over 68Ga-labeled tracers. It is being prepared with automated radiosynthesis machines within a short time frame (>20 min) with high yield (50-70%) and at room temperature (Wurzer et al., 2020). Radiosynthesis can be performed in accordance with good manufacturing practice. Batches can be prepared with activity that makes distribution to external PET-centres feasible. Additionally, the advantages of 18F lie in the possibility to produce it in larger quantities, the longer half-life, and a higher physical spatial resolution (Wurzer et al., 2020). The short half-life of 68Ga compared to 18F (68 vs. 110 min) makes 68Ga-PSMA unwieldy for longer transports. Thus, it is almost mandatory to use local gallium generators. These come with higher costs and lower yields at the end of their first half-life and each generator provides only one or two elutions per day and separate

syntheses are required at different times of the day in a local radio pharmacy (Pianou et al., 2019; Wurzer et al., 2020). However, compared with the literature, the results are not significantly better in diagnostics. The theranostic approach with rhPSMA ligands, including 18F-labelling, has potential for applications outside of early BCR. PSMA-directed radioligand-therapy could become a relevant application in relation to prostate cancer through pretherapeutic dosimetry using PET imaging with 18F (Hofman, Violet, et al., 2018; Wurzer et al., 2020).

5.1 Limitations

The still missing histopathological confirmation of the detected lesions, as in most studies of PSMA ligand PET imaging, and the well-known problem of the difficult biopsy of recurrent lesions in PC due to their small diameters play a major role in limitation of the study. Salvage therapy of choice is mostly local radiotherapy or ADT which subsequently does not provide much histological confirmation of the suspicious lesions. Ethically and logistically no such validation in patients with BCR after RP would be reasonable. However, in case of histopathological validation, the results confirmed the high positive predictive value of PSMA-based PET agents (Rauscher et al., 2017). Limitations of the study also lie in retrospectivity. As for all retrospective studies, the power is limited due to the lack of randomization and control groups and the higher risk of bias and increased susceptibility to error. Therefore, it lacks some potentially interesting information about the effects of PSA kinetics and patient outcomes but provides substantial evidence for planning urgently needed future prospective studies. The follow up of patients after imaging is not yet included in this study. Often, both the primary therapy and the further treatment took place in other hospitals than the Klinikum rechts der Isar and the resulting treatment inequality is an aggravating factor when it comes to the interpretation of the results.

A recently published study by Rauscher et. al. showed another pitfall that should not be disregarded. Here, the number of visually recognizable findings with increased PSMA ligand uptake, which could be attributed to a benign origin, was significantly higher with 18F-PSMA-1007-PET than with 68Ga-PSMA-11-PET. Thus, it is of great importance to parallel evaluate PET and CT

images as well as a sophisticated reading training to be in place and known pitfalls in the clinical context to be considered. Only in this way a reliable interpretation can be made (Rauscher et al., 2020).

6. Conclusion

Prostate cancer is the most common cancer in men and the incidence is also on the rise. Despite the ever-improving treatment methods, up to 35% of patients who underwent RP develop a BCR. For this situation, treatment options range from watchful waiting to systemic therapy or local surgery to salvage therapy. To be able to treat each patient optimally and individually, an exact and, in the best case, non-invasive restaging is of utmost importance. An imaging technique that sensitively and effectively shows the localization of carcinoma sites at very low PSA levels and early recurrence is desired, as this is the only way to enable successful therapy. As following RP, the PSA level is expected to be undetectable (< 0.1 ng/mL), PSA-threshold at relapse best predicting metastases after RP is > 0.4 ng/mL (Cornford et al., 2021; Mottet et al., 2017).

In this large population of 532 patients with recurrent prostate cancer after radical prostatectomy and a median PSA value of 0.97ng/mL (0.01-372ng/mL), a novel PSMA-based PET-tracer, 18F-rhPSMA-7, was used for PET/CT imaging. Pictures were evaluated by two independent doctors. One specialist for nuclear medicine and on specialist of radiology. All suspect lesions were noted.

The detection rates that were at least equal to data reported for 68Ga-PSMA-11, especially at low PSA values. The detection rate of 18F-rhPSMA-7 PET/CT is correlated positively with PSA levels and was 93.8% (150/160; 95% confidence interval [CI], 0.89–0.97) for a PSA value of ≥2 ng/mL, 85.3% (87/102; 95% CI, 0.77–0.92) for a PSA value of 1 to 2 ng/mL, 86.5% (90/104; 95% CI, 0.78–0.92) for a PSA value of 0.5 to 1 ng/mL, 63.8% (81/127; 95% CI,

0.55–0.72) for a PSA value of 0.2 to 0.5 ng/mL, and 38.5% (15/39; 95% CI, 0.23–0.55) for a PSA value of <0.2 ng/mL.

Except for the Gleason score, none of the other variables examined, such as ADT within the last six months before imaging or previously EBRT, showed a significant correlation with respect to detection rate.

Of greatest interest is the impact of the new rhPSMA imaging on the ongoing treatment strategy and associated better outcome.

DISCLOSURE

Hans-Juergen Wester, Alexander Wurzer, and Matthias Eiber are named as inventors on a patent application for rhPSMA. Hans-Juergen Wester and Matthias Eiber received funding from the SFB 824 (DFG Sonderforschungsbereich 824, project B11) from the Deutsche Forschungsgemeinschaft, Bonn, Germany, and from Blue Earth Diagnostics (licensee for rhPSMA) as part of an academic collaboration. Hans-Juergen Wester is a founder, shareholder, and advisory board member of Scintomics GmbH, Fuerstenfeldbruck, Germany. Matthias Eiber and Wolfgang Weber are consultants for Blue Earth Diagnostics. No other potential conflict of interest relevant to this article was reported.

References

Afshar-Oromieh, A., Debus, N., Uhrig, M., Hope, T. A., Evans, M. J., Holland-Letz, T., . . . Haberkorn, U. (2018). Impact of long-term androgen deprivation therapy on PSMA ligand PET/CT in patients with castration-sensitive prostate cancer. *Eur J Nucl Med Mol Imaging*, *45*(12), 2045-2054. https://doi.org/10.1007/s00259-018-4079-z

Afshar-Oromieh, A., Holland-Letz, T., Giesel, F. L., Kratochwil, C., Mier, W., Haufe, S., . . . Haberkorn, U. (2017). Diagnostic performance of (68)Ga-PSMA-11 (HBED-CC) PET/CT in patients with recurrent prostate cancer: evaluation in 1007 patients. *Eur J Nucl Med Mol Imaging*, *44*(8), 1258-1268. https://doi.org/10.1007/s00259-017-3711-7

Aggarwal, R., Wei, X., Kim, W., Small, E. J., Ryan, C. J., Carroll, P., . . . Hope, T. (2018). Heterogeneous Flare in Prostate-specific Membrane Antigen Positron Emission Tomography Tracer Uptake with Initiation of Androgen Pathway Blockade in Metastatic Prostate Cancer. *Eur Urol Oncol*, *1*(1), 78-82. https://doi.org/10.1016/j.euo.2018.03.010

Andriole, G. L., Kostakoglu, L., Chau, A., Duan, F., Mahmood, U., Mankoff, D. A., . . . Siegel, B. A. (2019). The Impact of Positron Emission Tomography with 18F-Fluciclovine on the Treatment of Biochemical Recurrence of Prostate Cancer: Results from the LOCATE Trial. *J Urol*, *201*(2), 322-331. https://doi.org/10.1016/j.juro.2018.08.050

Baade, P. D., Youlden, D. R., & Krnjacki, L. J. (2009). International epidemiology of prostate cancer: geographical distribution and secular trends. *Mol Nutr Food Res*, *53*(2), 171-184. https://doi.org/10.1002/mnfr.200700511

Barbosa, F. G., Queiroz, M. A., Nunes, R. F., Viana, P. C. C., Marin, J. F. G., Cerri, G. G., & Buchpiguel, C. A. (2019). Revisiting Prostate Cancer Recurrence with PSMA PET: Atlas of Typical and Atypical Patterns of Spread. *Radiographics*, *39*(1), 186-212. https://doi.org/10.1148/rg.2019180079

Barinka, C., Sácha, P., Sklenár, J., Man, P., Bezouska, K., Slusher, B. S., & Konvalinka, J. (2004). Identification of the N-glycosylation sites on glutamate carboxypeptidase II necessary for proteolytic activity. *Protein Sci*, *13*(6), 1627-1635. https://doi.org/10.1110/ps.04622104

Bravaccini, S., Puccetti, M., Bocchini, M., Ravaioli, S., Celli, M., Scarpi, E., . . . Paganelli, G. (2018). PSMA expression: a potential ally for the pathologist in prostate cancer diagnosis. *Scientific Reports*, *8*(1), 4254. https://doi.org/10.1038/s41598-018-22594-1

Bray, F., Ferlay, J., Soerjomataram, I., Siegel, R. L., Torre, L. A., & Jemal, A. (2018). Global cancer statistics 2018: GLOBOCAN estimates of incidence and mortality worldwide for 36 cancers

in 185 countries. *CA Cancer J Clin*, *68*(6), 394-424. https://doi.org/10.3322/caac.21492

Castellucci, P., Fuccio, C., Nanni, C., Santi, I., Rizzello, A., Lodi, F., . . . Fanti, S. (2009). Influence of trigger PSA and PSA kinetics on 11C-Choline PET/CT detection rate in patients with biochemical relapse after radical prostatectomy. *J Nucl Med*, *50*(9), 1394-1400. https://doi.org/10.2967/jnumed.108.061507

Catalona, W. J., Richie, J. P., Ahmann, F. R., Hudson, M. A., Scardino, P. T., Flanigan, R. C., . . . Southwick, P. C. (1994). Comparison of digital rectal examination and serum prostate specific antigen in the early detection of prostate cancer: results of a multicenter clinical trial of 6,630 men. *J Urol*, *151*(5), 1283-1290. https://doi.org/10.1016/s0022-5347(17)35233-3

Chakravarty, R., Siamof, C. M., Dash, A., & Cai, W. (2018). Targeted α-therapy of prostate cancer using radiolabeled PSMA inhibitors: a game changer in nuclear medicine. *Am J Nucl Med Mol Imaging*, *8*(4), 247-267.

Chen, M., Zhang, Q., Zhang, C., Zhou, Y. H., Zhao, X., Fu, Y., . . . Guo, H. (2020). Comparison of (68)Ga-prostate-specific membrane antigen (PSMA) positron emission tomography/computed tomography (PET/CT) and multi-parametric magnetic resonance imaging (MRI) in the evaluation of tumor extension of primary prostate cancer. *Transl Androl Urol*, *9*(2), 382-390. https://doi.org/10.21037/tau.2020.03.06

Christiansen, J. J., Rajasekaran, S. A., Inge, L., Cheng, L., Anilkumar, G., Bander, N. H., & Rajasekaran, A. K. (2005). N-glycosylation and microtubule integrity are involved in apical targeting of prostate-specific membrane antigen: implications for immunotherapy. *Mol Cancer Ther*, *4*(5), 704-714. https://doi.org/10.1158/1535-7163.Mct-04-0171

Chu, C. E., Alshalalfa, M., Sjostrom, M., Zhao, S. G., Liu, Y., Chou, J., . . . Feng, F. Y. (2021). Prostate-specific Membrane Antigen and Fluciclovine Transporter Genes are Associated with Variable Clinical Features and Molecular Subtypes of Primary Prostate Cancer. *Eur Urol*, *79*(6), 717-721. https://doi.org/10.1016/j.eururo.2021.03.017

Cornford, P., Bellmunt, J., Bolla, M., Briers, E., De Santis, M., Gross, T., . . . Mottet, N. (2017). EAU-ESTRO-SIOG Guidelines on Prostate Cancer. Part II: Treatment of Relapsing, Metastatic, and Castration-Resistant Prostate Cancer. *Eur Urol*, *71*(4), 630-642. https://doi.org/10.1016/j.eururo.2016.08.002

Cornford, P., van den Bergh, R. C. N., Briers, E., Van den Broeck, T., Cumberbatch, M. G., De Santis, M., . . . Mottet, N. (2021). EAU-EANM-ESTRO-ESUR-SIOG Guidelines on Prostate Cancer. Part II-2020 Update: Treatment of Relapsing and Metastatic

Prostate Cancer. *Eur Urol*, *79*(2), 263-282. https://doi.org/10.1016/j.eururo.2020.09.046

Dietlein, F., Kobe, C., Neubauer, S., Schmidt, M., Stockter, S., Fischer, T., . . . Dietlein, M. (2017). PSA-Stratified Performance of ¹⁸F- and ⁶⁸Ga-PSMA PET in Patients with Biochemical Recurrence of Prostate Cancer. *Journal of Nuclear Medicine*, *58*(6), 947-952. https://doi.org/10.2967/jnumed.116.185538

Ding, P., Helquist, P., & Miller, M. J. (2007). Design, synthesis and pharmacological activity of novel enantiomerically pure phosphonic acid-based NAALADase inhibitors. *Org Biomol Chem*, *5*(5), 826-831. https://doi.org/10.1039/b615603g

Duwel, C., Eiber, M., & Maurer, T. (2016). [Will 68Ga-PSMA PET become the New Imaging Standard for Prostate Cancer?]. *Aktuelle Urol*, *47*(5), 378-382. https://doi.org/10.1055/s-0042-110982 (68Ga-PSMA PET auf dem Weg zur neuen Standardbildgebung bei Prostatakarzinom?)

Eiber, M., Fendler, W. P., Rowe, S. P., Calais, J., Hofman, M. S., Maurer, T., . . . Giesel, F. L. (2017). Prostate-Specific Membrane Antigen Ligands for Imaging and Therapy. *J Nucl Med*, *58*(Suppl 2), 67S-76S. https://doi.org/10.2967/jnumed.116.186767

Eiber, M., Maurer, T., Souvatzoglou, M., Beer, A. J., Ruffani, A., Haller, B., . . . Schwaiger, M. (2015). Evaluation of Hybrid (6)(8)Ga-PSMA Ligand PET/CT in 248 Patients with Biochemical Recurrence After Radical Prostatectomy. *J Nucl Med*, *56*(5), 668-674. https://doi.org/10.2967/jnumed.115.154153

Emmett, L., van Leeuwen, P. J., Nandurkar, R., Scheltema, M. J., Cusick, T., Hruby, G., . . . Stricker, P. (2017). Treatment Outcomes from (68)Ga-PSMA PET/CT-Informed Salvage Radiation Treatment in Men with Rising PSA After Radical Prostatectomy: Prognostic Value of a Negative PSMA PET. *J Nucl Med*, *58*(12), 1972-1976. https://doi.org/10.2967/jnumed.117.196683

Emmett, L., Yin, C., Crumbaker, M., Hruby, G., Kneebone, A., Epstein, R., . . . Joshua, A. M. (2019). Rapid Modulation of PSMA Expression by Androgen Deprivation: Serial (68)Ga-PSMA-11 PET in Men with Hormone-Sensitive and Castrate-Resistant Prostate Cancer Commencing Androgen Blockade. *J Nucl Med*, *60*(7), 950-954. https://doi.org/10.2967/jnumed.118.223099

Epstein, J. I., Allsbrook, W. C., Jr., Amin, M. B., & Egevad, L. L. (2005). The 2005 International Society of Urological Pathology (ISUP) Consensus Conference on Gleason Grading of Prostatic Carcinoma. *Am J Surg Pathol*, *29*(9), 1228-1242. https://doi.org/10.1097/01.pas.0000173646.99337.b1

Ettala, O., Malaspina, S., Tuokkola, T., Luoto, P., Löyttyniemi, E., Boström, P. J., & Kemppainen, J. (2020). Prospective study on

the effect of short-term androgen deprivation therapy on PSMA uptake evaluated with (68)Ga-PSMA-11 PET/MRI in men with treatment-naïve prostate cancer. *Eur J Nucl Med Mol Imaging*, *47*(3), 665-673. https://doi.org/10.1007/s00259-019-04635-7

Fernández-García, E. M., Vera-Badillo, F. E., Perez-Valderrama, B., Matos-Pita, A. S., & Duran, I. (2015). Immunotherapy in prostate cancer: review of the current evidence. *Clin Transl Oncol*, *17*(5), 339-357. https://doi.org/10.1007/s12094-014-1259-6

Fossati, N., Karnes, R. J., Cozzarini, C., Fiorino, C., Gandaglia, G., Joniau, S., . . . Briganti, A. (2016). Assessing the Optimal Timing for Early Salvage Radiation Therapy in Patients with Prostate-specific Antigen Rise After Radical Prostatectomy. *Eur Urol*, *69*(4), 728-733. https://doi.org/10.1016/j.eururo.2015.10.009

Freitag, M. T., Radtke, J. P., Hadaschik, B. A., Kopp-Schneider, A., Eder, M., Kopka, K., . . . Afshar-Oromieh, A. (2016). Comparison of hybrid (68)Ga-PSMA PET/MRI and (68)Ga-PSMA PET/CT in the evaluation of lymph node and bone metastases of prostate cancer. *Eur J Nucl Med Mol Imaging*, *43*(1), 70-83. https://doi.org/10.1007/s00259-015-3206-3

Giesel, F. L., Cardinale, J., Schäfer, M., Neels, O., Benešová, M., Mier, W., . . . Kratochwil, C. (2016). (18)F-Labelled PSMA-1007 shows similarity in structure, biodistribution and tumour uptake to the theragnostic compound PSMA-617. *Eur J Nucl Med Mol Imaging*, *43*(10), 1929-1930. https://doi.org/10.1007/s00259-016-3447-9

Giesel, F. L., Hadaschik, B., Cardinale, J., Radtke, J., Vinsensia, M., Lehnert, W., . . . Kratochwil, C. (2017). F-18 labelled PSMA-1007: biodistribution, radiation dosimetry and histopathological validation of tumor lesions in prostate cancer patients. *Eur J Nucl Med Mol Imaging*, *44*(4), 678-688. https://doi.org/10.1007/s00259-016-3573-4

Giesel, F. L., Knorr, K., Spohn, F., Will, L., Maurer, T., Flechsig, P., . . . Eiber, M. (2019). Detection Efficacy of (18)F-PSMA-1007 PET/CT in 251 Patients with Biochemical Recurrence of Prostate Cancer After Radical Prostatectomy. *J Nucl Med*, *60*(3), 362-368. https://doi.org/10.2967/jnumed.118.212233

Giesel, F. L., Will, L., Lawal, I., Lengana, T., Kratochwil, C., Vorster, M., . . . Sathekge, M. (2018). Intraindividual Comparison of (18)F-PSMA-1007 and (18)F-DCFPyL PET/CT in the Prospective Evaluation of Patients with Newly Diagnosed Prostate Carcinoma: A Pilot Study. *J Nucl Med*, *59*(7), 1076-1080. https://doi.org/10.2967/jnumed.117.204669

Glatting, G., Wängler, C., & Wängler, B. (2017). Physikalisch-technische Grundlagen und Tracerentwicklung in der Positronenemissionstomografie. In U. Attenberger, M. Ritter, &

F. Wenz (Eds.), *MR- und PET-Bildgebung der Prostata: Diagnostik und Therapieplanung* (pp. 19-56). Springer Berlin Heidelberg. https://doi.org/10.1007/978-3-662-50468-0_2

Goldstein, J., Even-Sapir, E., Ben-Haim, S., Saad, A., Spieler, B., Davidson, T., . . . Symon, Z. (2017). Does Choline PET/CT Change the Management of Prostate Cancer Patients With Biochemical Failure? *Am J Clin Oncol*, *40*(3), 256-259. https://doi.org/10.1097/coc.0000000000000139

Gorin, M. A., Rowe, S. P., Patel, H. D., Vidal, I., Mana-Ay, M., Javadi, M. S., . . . Allaf, M. E. (2018). Prostate Specific Membrane Antigen Targeted (18)F-DCFPyL Positron Emission Tomography/Computerized Tomography for the Preoperative Staging of High Risk Prostate Cancer: Results of a Prospective, Phase II, Single Center Study. *J Urol*, *199*(1), 126-132. https://doi.org/10.1016/j.juro.2017.07.070

Haberkorn, U., Eder, M., Kopka, K., Babich, J. W., & Eisenhut, M. (2016). New Strategies in Prostate Cancer: Prostate-Specific Membrane Antigen (PSMA) Ligands for Diagnosis and Therapy. *Clinical Cancer Research*, *22*(1), 9-15. https://doi.org/10.1158/1078-0432.Ccr-15-0820

Han, S., Woo, S., Kim, Y. J., & Suh, C. H. (2018). Impact of (68)Ga-PSMA PET on the Management of Patients with Prostate Cancer: A Systematic Review and Meta-analysis. *Eur Urol*, *74*(2), 179-190. https://doi.org/10.1016/j.eururo.2018.03.030

Henninger, M., Maurer, T., Hacker, C., & Eiber, M. (2016). 68Ga-PSMA PET/MR Showing Intense PSMA Uptake in Nodular Fasciitis Mimicking Prostate Cancer Metastasis. *Clin Nucl Med*, *41*(10), e443-444. https://doi.org/10.1097/RLU.0000000000001310

Hentschel, M., Paul, D., Moser, E., & Brink, I. (2007). Möglichkeiten und Grenzen der modernen Schnittbildverfahren (CT, MRT, PET) in der molekularen Bildgebung. *Der Nuklearmediziner*, *30*, 31-41. https://doi.org/10.1055/s-2006-955216

Hofman, M. S., Emmett, L., Violet, J., A, Y. Z., Lawrence, N. J., Stockler, M., . . . Davis, I. D. (2019). TheraP: a randomized phase 2 trial of (177) Lu-PSMA-617 theranostic treatment vs cabazitaxel in progressive metastatic castration-resistant prostate cancer (Clinical Trial Protocol ANZUP 1603). *BJU Int*, *124 Suppl 1*, 5-13. https://doi.org/10.1111/bju.14876

Hofman, M. S., Hicks, R. J., Maurer, T., & Eiber, M. (2018). Prostate-specific Membrane Antigen PET: Clinical Utility in Prostate Cancer, Normal Patterns, Pearls, and Pitfalls. *Radiographics*, *38*(1), 200-217. https://doi.org/10.1148/rg.2018170108

Hofman, M. S., Violet, J., Hicks, R. J., Ferdinandus, J., Thang, S. P., Akhurst, T., . . . Sandhu, S. (2018). [(177)Lu]-PSMA-617 radionuclide treatment in patients with metastatic castration-resistant prostate cancer (LuPSMA trial): a single-centre,

single-arm, phase 2 study. *Lancet Oncol*, *19*(6), 825-833. https://doi.org/10.1016/s1470-2045(18)30198-0

Hofmann, M., Maecke, H., Börner, R., Weckesser, E., Schöffski, P., Oei, L., . . . Knapp, H. (2001). Biokinetics and imaging with the somatostatin receptor PET radioligand (68)Ga-DOTATOC: preliminary data. *Eur J Nucl Med*, *28*(12), 1751-1757. https://doi.org/10.1007/s002590100639

Holland, J. P., Divilov, V., Bander, N. H., Smith-Jones, P. M., Larson, S. M., & Lewis, J. S. (2010). 89Zr-DFO-J591 for immunoPET of prostate-specific membrane antigen expression in vivo. *J Nucl Med*, *51*(8), 1293-1300. https://doi.org/10.2967/jnumed.110.076174

Hope, T. A., Truillet, C., Ehman, E. C., Afshar-Oromieh, A., Aggarwal, R., Ryan, C. J., . . . Evans, M. J. (2017). 68Ga-PSMA-11 PET Imaging of Response to Androgen Receptor Inhibition: First Human Experience. *J Nucl Med*, *58*(1), 81-84. https://doi.org/10.2967/jnumed.116.181800

Horoszewicz, J. S., Kawinski, E., & Murphy, G. P. (1987). Monoclonal antibodies to a new antigenic marker in epithelial prostatic cells and serum of prostatic cancer patients. *Anticancer Res*, *7*(5b), 927-935.

Hövels, A. M., Heesakkers, R. A., Adang, E. M., Jager, G. J., Strum, S., Hoogeveen, Y. L., . . . Barentsz, J. O. (2008). The diagnostic accuracy of CT and MRI in the staging of pelvic lymph nodes in patients with prostate cancer: a meta-analysis. *Clin Radiol*, *63*(4), 387-395. https://doi.org/10.1016/j.crad.2007.05.022

Jackson, P. F., Cole, D. C., Slusher, B. S., Stetz, S. L., Ross, L. E., Donzanti, B. A., & Trainor, D. A. (1996). Design, synthesis, and biological activity of a potent inhibitor of the neuropeptidase N-acetylated alpha-linked acidic dipeptidase. *J Med Chem*, *39*(2), 619-622. https://doi.org/10.1021/jm950801q

Janssen, J. C., Meißner, S., Woythal, N., Prasad, V., Brenner, W., Diederichs, G., . . . Makowski, M. R. (2018). Comparison of hybrid (68)Ga-PSMA-PET/CT and (99m)Tc-DPD-SPECT/CT for the detection of bone metastases in prostate cancer patients: Additional value of morphologic information from low dose CT. *Eur Radiol*, *28*(2), 610-619. https://doi.org/10.1007/s00330-017-4994-6

Jilg, C. A., Drendel, V., Rischke, H. C., Beck, T., Vach, W., Schaal, K., . . . Meyer, P. T. (2017). Diagnostic Accuracy of Ga-68-HBED-CC-PSMA-Ligand-PET/CT before Salvage Lymph Node Dissection for Recurrent Prostate Cancer [Research Paper]. *Theranostics*, *7*(6), 1770-1780. https://doi.org/10.7150/thno.18421

Jochumsen, M. R., Dias, A. H., & Bouchelouche, K. (2018). Benign Traumatic Rib Fracture: A Potential Pitfall on 68Ga-Prostate-Specific Membrane Antigen PET/CT for Prostate Cancer. *Clin*

Nucl Med, *43*(1), 38-40. https://doi.org/10.1097/rlu.0000000000001871
Kane, C. J., Amling, C. L., Johnstone, P. A., Pak, N., Lance, R. S., Thrasher, J. B., . . . Moul, J. W. (2003). Limited value of bone scintigraphy and computed tomography in assessing biochemical failure after radical prostatectomy. *Urology*, *61*(3), 607-611. https://doi.org/10.1016/s0090-4295(02)02411-1
Karyagar, S. S., Karyagar, S., & Guven, O. (2020). Correlations of the (68)Ga-PSMA PET/CT derived primary prostate tumor PSMA expression parameters and metastatic patterns in patients with Gleason Score >7 prostate cancer. *Hell J Nucl Med*, *23*(2), 120-124. https://doi.org/10.1967/s002449912100
Kroenke, M., Wurzer, A., Schwamborn, K., Ulbrich, L., JooÃŸ, L., Maurer, T., . . . Eiber, M. (2019). Histologically-confirmed diagnostic efficacy of 18F-rhPSMA-7 positron emission tomography for N-staging of patients with high risk primary prostate cancer. *Journal of Nuclear Medicine*, *60*(supplement 1), 1567.
Kvåle, R., Myklebust, T., Fosså, S. D., Aas, K., Ekanger, C., Helle, S. I., . . . Møller, B. (2019). Impact of positive surgical margins on secondary treatment, palliative radiotherapy and prostate cancer-specific mortality. A population-based study of 13 198 patients. *Prostate*, *79*(16), 1852-1860. https://doi.org/10.1002/pros.23911
Leitsmann, C., Thelen, P., Schmid, M., Meller, J., Sahlmann, C.-O., Meller, B., . . . Strauss, A. (2019). Enhancing PSMA-uptake with androgen deprivation therapy - a new way to detect prostate cancer metastases? *International braz j urol : official journal of the Brazilian Society of Urology*, *45*(3), 459-467. https://doi.org/10.1590/s1677-5538.ibju.2018.0305
Lin, M., Ta, R. T., Kairemo, K., Le, D. B., & Ravizzini, G. C. (2020). Prostate-Specific Membrane Antigen-Targeted Radiopharmaceuticals in Diagnosis and Therapy of Prostate Cancer: Current Status and Future Perspectives. *Cancer Biother Radiopharm*. https://doi.org/10.1089/cbr.2020.3603
Lindenberg, L., Choyke, P., & Dahut, W. (2016). Prostate Cancer Imaging with Novel PET Tracers. *Curr Urol Rep*, *17*(3), 18. https://doi.org/10.1007/s11934-016-0575-5
Maurer, T., Eiber, M., Schwaiger, M., & Gschwend, J. E. (2016). Current use of PSMA-PET in prostate cancer management. *Nat Rev Urol*, *13*(4), 226-235. https://doi.org/10.1038/nrurol.2016.26
Maurer, T., Gschwend, J. E., Rauscher, I., Souvatzoglou, M., Haller, B., Weirich, G., . . . Eiber, M. (2016). Diagnostic Efficacy of (68)Gallium-PSMA Positron Emission Tomography Compared to Conventional Imaging for Lymph Node Staging of 130 Consecutive Patients with Intermediate to High Risk Prostate

Cancer. *J Urol*, *195*(5), 1436-1443. https://doi.org/10.1016/j.juro.2015.12.025
Meller, B., Bremmer, F., Sahlmann, C. O., Hijazi, S., Bouter, C., Trojan, L., . . . Thelen, P. (2015). Alterations in androgen deprivation enhanced prostate-specific membrane antigen (PSMA) expression in prostate cancer cells as a target for diagnostics and therapy. *EJNMMI Research*, *5*(1), 66. https://doi.org/10.1186/s13550-015-0145-8
Mottet, N., Bellmunt, J., Bolla, M., Briers, E., Cumberbatch, M. G., De Santis, M., . . . Cornford, P. (2017). EAU-ESTRO-SIOG Guidelines on Prostate Cancer. Part 1: Screening, Diagnosis, and Local Treatment with Curative Intent. *Eur Urol*, *71*(4), 618-629. https://doi.org/10.1016/j.eururo.2016.08.003
Mottet, N., Bellmunt, J., Bolla, M., Joniau, S., Mason, M., Matveev, V., . . . Heidenreich, A. (2011). EAU guidelines on prostate cancer. Part II: Treatment of advanced, relapsing, and castration-resistant prostate cancer. *Eur Urol*, *59*(4), 572-583. https://doi.org/10.1016/j.eururo.2011.01.025
Onal, C., Guler, O. C., Torun, N., Reyhan, M., & Yapar, A. F. (2020). The effect of androgen deprivation therapy on (68)Ga-PSMA tracer uptake in non-metastatic prostate cancer patients. *Eur J Nucl Med Mol Imaging*, *47*(3), 632-641. https://doi.org/10.1007/s00259-019-04581-4
Perera, M., Papa, N., Christidis, D., Wetherell, D., Hofman, M. S., Murphy, D. G., . . . Lawrentschuk, N. (2016). Sensitivity, Specificity, and Predictors of Positive (68)Ga-Prostate-specific Membrane Antigen Positron Emission Tomography in Advanced Prostate Cancer: A Systematic Review and Meta-analysis. *Eur Urol*, *70*(6), 926-937. https://doi.org/10.1016/j.eururo.2016.06.021
Perera, M., Papa, N., Roberts, M., Williams, M., Udovicich, C., Vela, I., . . . Murphy, D. G. (2020). Gallium-68 Prostate-specific Membrane Antigen Positron Emission Tomography in Advanced Prostate Cancer-Updated Diagnostic Utility, Sensitivity, Specificity, and Distribution of Prostate-specific Membrane Antigen-avid Lesions: A Systematic Review and Meta-analysis. *Eur Urol*, *77*(4), 403-417. https://doi.org/10.1016/j.eururo.2019.01.049
Petronis, J. D., Regan, F., & Lin, K. (1998). Indium-111 capromab pendetide (ProstaScint) imaging to detect recurrent and metastatic prostate cancer. *Clin Nucl Med*, *23*(10), 672-677. https://doi.org/10.1097/00003072-199810000-00005
Pfister, D., Bolla, M., Briganti, A., Carroll, P., Cozzarini, C., Joniau, S., . . . Zelefsky, M. J. (2014). Early salvage radiotherapy following radical prostatectomy. *Eur Urol*, *65*(6), 1034-1043. https://doi.org/10.1016/j.eururo.2013.08.013
Pianou, N. K., Stavrou, P. Z., Vlontzou, E., Rondogianni, P., Exarhos, D. N., & Datseris, I. E. (2019). More advantages in detecting

bone and soft tissue metastases from prostate cancer using (18)F-PSMA PET/CT. *Hell J Nucl Med*, *22*(1), 6-9. https://doi.org/10.1967/s002449910952

Rahbar, K., Afshar-Oromieh, A., Seifert, R., Wagner, S., Schäfers, M., Bögemann, M., & Weckesser, M. (2018). Diagnostic performance of (18)F-PSMA-1007 PET/CT in patients with biochemical recurrent prostate cancer. *Eur J Nucl Med Mol Imaging*, *45*(12), 2055-2061. https://doi.org/10.1007/s00259-018-4089-x

Rahbar, K., Weckesser, M., Ahmadzadehfar, H., Schäfers, M., Stegger, L., & Bögemann, M. (2018). Advantage of (18)F-PSMA-1007 over (68)Ga-PSMA-11 PET imaging for differentiation of local recurrence vs. urinary tracer excretion. *Eur J Nucl Med Mol Imaging*, *45*(6), 1076-1077. https://doi.org/10.1007/s00259-018-3952-0

Rahman, L. A., Rutagengwa, D., Lin, P., Lin, M., Yap, J., Lai, K., . . . Lalak, N. (2019). High negative predictive value of 68Ga PSMA PET-CT for local lymph node metastases in high risk primary prostate cancer with histopathological correlation. *Cancer Imaging*, *19*(1), 86. https://doi.org/10.1186/s40644-019-0273-x

Rauscher, I., Duwel, C., Wirtz, M., Schottelius, M., Wester, H. J., Schwamborn, K., . . . Maurer, T. (2017). Value of (111) In-prostate-specific membrane antigen (PSMA)-radioguided surgery for salvage lymphadenectomy in recurrent prostate cancer: correlation with histopathology and clinical follow-up. *BJU Int*, *120*(1), 40-47. https://doi.org/10.1111/bju.13713

Rauscher, I., Krönke, M., König, M., Gafita, A., Maurer, T., Horn, T., . . . Eiber, M. (2020). Matched-Pair Comparison of (68)Ga-PSMA-11 PET/CT and (18)F-PSMA-1007 PET/CT: Frequency of Pitfalls and Detection Efficacy in Biochemical Recurrence After Radical Prostatectomy. *J Nucl Med*, *61*(1), 51-57. https://doi.org/10.2967/jnumed.119.229187

Rawla, P. (2019). Epidemiology of Prostate Cancer. *World J Oncol*, *10*(2), 63-89. https://doi.org/10.14740/wjon1191

Ross, J. S., Sheehan, C. E., Fisher, H. A., Kaufman, R. P., Jr., Kaur, P., Gray, K., . . . Kallakury, B. V. (2003). Correlation of primary tumor prostate-specific membrane antigen expression with disease recurrence in prostate cancer. *Clin Cancer Res*, *9*(17), 6357-6362.

Roy, J., White, M. E., Basuli, F., Opina, A. C. L., Wong, K., Riba, M., . . . Jagoda, E. M. (2021). Monitoring PSMA Responses to ADT in Prostate Cancer Patient-Derived Xenograft Mouse Models Using [(18)F]DCFPyL PET Imaging. *Mol Imaging Biol*, *23*(5), 745-755. https://doi.org/10.1007/s11307-021-01605-0

Sanchez-Crespo, A. (2013). Comparison of Gallium-68 and Fluorine-18 imaging characteristics in positron emission tomography.

Appl Radiat Isot, *76*, 55-62. https://doi.org/10.1016/j.apradiso.2012.06.034

Sargos, P., Chabaud, S., Latorzeff, I., Magné, N., Benyoucef, A., Supiot, S., . . . Richaud, P. (2020). Adjuvant radiotherapy versus early salvage radiotherapy plus short-term androgen deprivation therapy in men with localised prostate cancer after radical prostatectomy (GETUG-AFU 17): a randomised, phase 3 trial. *Lancet Oncol*, *21*(10), 1341-1352. https://doi.org/10.1016/s1470-2045(20)30454-x

Sheikhbahaei, S., Afshar-Oromieh, A., Eiber, M., Solnes, L. B., Javadi, M. S., Ross, A. E., . . . Rowe, S. P. (2017). Pearls and pitfalls in clinical interpretation of prostate-specific membrane antigen (PSMA)-targeted PET imaging. *Eur J Nucl Med Mol Imaging*, *44*(12), 2117-2136. https://doi.org/10.1007/s00259-017-3780-7

Smith-Jones, P. M., Vallabhajosula, S., Navarro, V., Bastidas, D., Goldsmith, S. J., & Bander, N. H. (2003). Radiolabeled monoclonal antibodies specific to the extracellular domain of prostate-specific membrane antigen: preclinical studies in nude mice bearing LNCaP human prostate tumor. *J Nucl Med*, *44*(4), 610-617.

Sodee, D. B., Malguria, N., Faulhaber, P., Resnick, M. I., Albert, J., & Bakale, G. (2000). Multicenter ProstaScint imaging findings in 2154 patients with prostate cancer. The ProstaScint Imaging Centers. *Urology*, *56*(6), 988-993. https://doi.org/10.1016/s0090-4295(00)00824-4

Stephenson, A. J., Kattan, M. W., Eastham, J. A., Dotan, Z. A., Bianco, F. J., Jr., Lilja, H., & Scardino, P. T. (2006). Defining biochemical recurrence of prostate cancer after radical prostatectomy: a proposal for a standardized definition. *J Clin Oncol*, *24*(24), 3973-3978. https://doi.org/10.1200/jco.2005.04.0756

Sterzing, F., Kratochwil, C., Fiedler, H., Katayama, S., Habl, G., Kopka, K., . . . Giesel, F. L. (2016). (68)Ga-PSMA-11 PET/CT: a new technique with high potential for the radiotherapeutic management of prostate cancer patients. *Eur J Nucl Med Mol Imaging*, *43*(1), 34-41. https://doi.org/10.1007/s00259-015-3188-1

Stish, B. J., Pisansky, T. M., Harmsen, W. S., Davis, B. J., Tzou, K. S., Choo, R., & Buskirk, S. J. (2016). Improved Metastasis-Free and Survival Outcomes With Early Salvage Radiotherapy in Men With Detectable Prostate-Specific Antigen After Prostatectomy for Prostate Cancer. *J Clin Oncol*, *34*(32), 3864-3871. https://doi.org/10.1200/jco.2016.68.3425

Troyer, J. K., Beckett, M. L., & Wright, G. L., Jr. (1995). Detection and characterization of the prostate-specific membrane antigen (PSMA) in tissue extracts and body fluids. *Int J Cancer*, *62*(5), 552-558. https://doi.org/10.1002/ijc.2910620511

Troyer, J. K., Beckett, M. L., & Wright, G. L., Jr. (1997). Location of prostate-specific membrane antigen in the LNCaP prostate carcinoma cell line. *Prostate*, *30*(4), 232-242. https://doi.org/10.1002/(sici)1097-0045(19970301)30:4<232::aid-pros2>3.0.co;2-n

Van den Broeck, T., van den Bergh, R. C. N., Briers, E., Cornford, P., Cumberbatch, M., Tilki, D., . . . Mottet, N. (2019). Biochemical Recurrence in Prostate Cancer: The European Association of Urology Prostate Cancer Guidelines Panel Recommendations. *Eur Urol Focus*. https://doi.org/10.1016/j.euf.2019.06.004

Van den Broeck, T., van den Bergh, R. C. N., Briers, E., Cornford, P., Cumberbatch, M., Tilki, D., . . . Mottet, N. (2020). Biochemical Recurrence in Prostate Cancer: The European Association of Urology Prostate Cancer Guidelines Panel Recommendations. *Eur Urol Focus*, *6*(2), 231-234. https://doi.org/10.1016/j.euf.2019.06.004

Wiegel, T., Lohm, G., Bottke, D., Höcht, S., Miller, K., Siegmann, A., . . . Hinkelbein, W. (2009). Achieving an undetectable PSA after radiotherapy for biochemical progression after radical prostatectomy is an independent predictor of biochemical outcome--results of a retrospective study. *Int J Radiat Oncol Biol Phys*, *73*(4), 1009-1016. https://doi.org/10.1016/j.ijrobp.2008.06.1922

Witkowska-Patena, E., Giżewska, A., Dziuk, M., Miśko, J., Budzyńska, A., & Walęcka-Mazur, A. (2020). Diagnostic performance of 18F-PSMA-1007 PET/CT in biochemically relapsed patients with prostate cancer with PSA levels ≤ 2.0 ng/ml. *Prostate Cancer Prostatic Dis*, *23*(2), 343-348. https://doi.org/10.1038/s41391-019-0194-6

Wright, G. L., Jr., Grob, B. M., Haley, C., Grossman, K., Newhall, K., Petrylak, D., . . . Moriarty, R. (1996). Upregulation of prostate-specific membrane antigen after androgen-deprivation therapy. *Urology*, *48*(2), 326-334. https://doi.org/10.1016/s0090-4295(96)00184-7

Wurzer, A., Di Carlo, D., Schmidt, A., Beck, R., Eiber, M., Schwaiger, M., & Wester, H. J. (2020). Radiohybrid Ligands: A Novel Tracer Concept Exemplified by (18)F- or (68)Ga-Labeled rhPSMA Inhibitors. *J Nucl Med*, *61*(5), 735-742. https://doi.org/10.2967/jnumed.119.234922